TNO report
PML 1998-A80

Trajectory Simulation Model for a Side-Thruster Guided MLRS-Type Vehicle

TNO Prins Maurits Laboratory

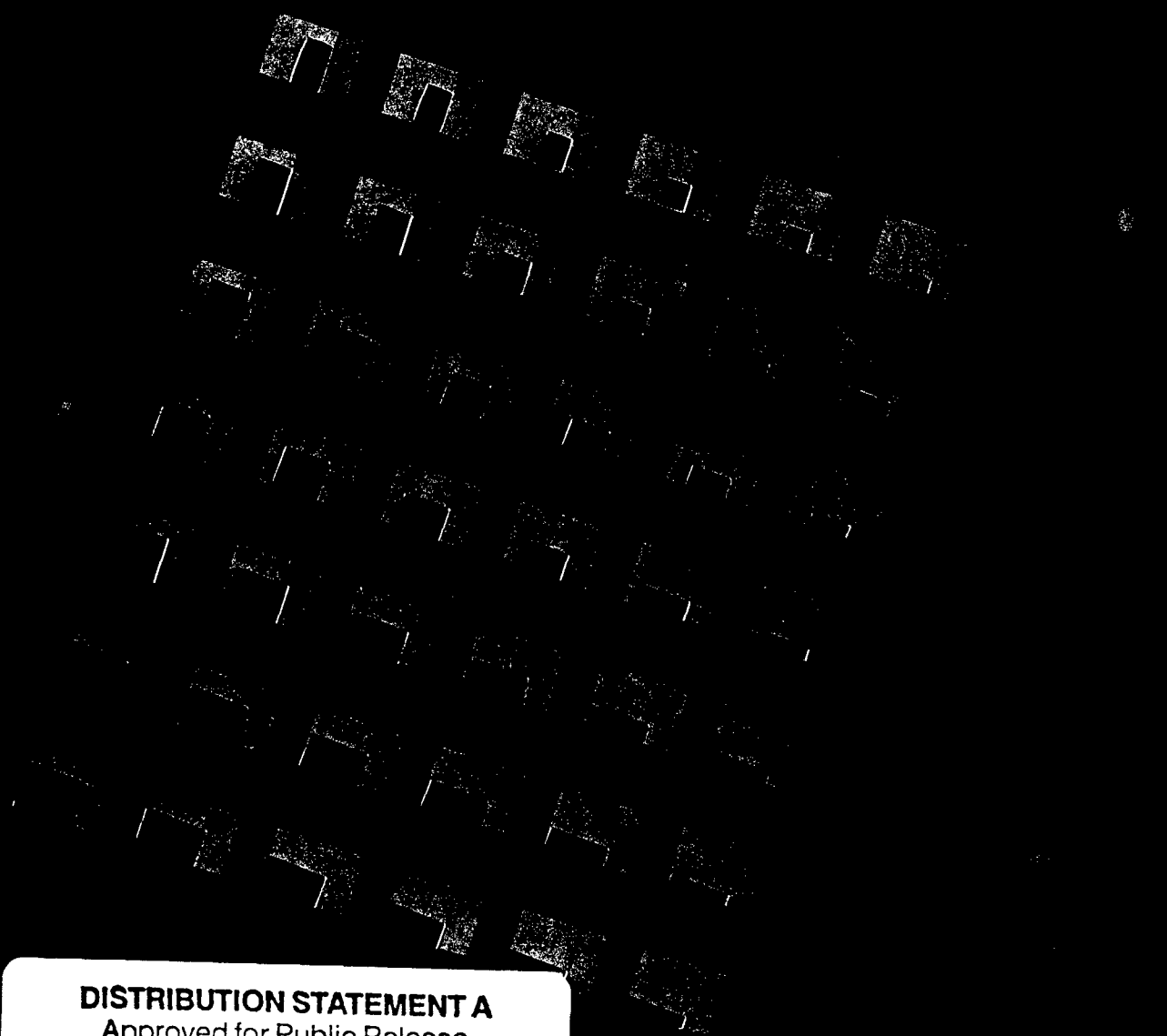

TNO

TNO report
PML 1998-A80

Trajectory Simulation Model for a Side-Thruster Guided MLRS-Type Vehicle

TNO Prins Maurits Laboratory

Lange Kleiweg 137
P.O. Box 45
2280 AA Rijswijk
The Netherlands

Phone +31 15 284 28 42
Fax +31 15 284 39 58

Date
May 1999

Author(s)
Dr. G.M.H.J.L. Gadiot

Classification		
Classified by	:	Major J. Kerkvliet
Classification date	:	6 April 1999
		(after 10 years this classification is no longer valid)
Title	:	Ongerubriceerd
Managementuittreksel	:	Ongerubriceerd
Abstract	:	Ongerubriceerd
Report text	:	Ongerubriceerd

Copy no.	:	13
No. of copies	:	23
No. of pages	:	45 (excl. RDP & distribution list)
No. of annexes	:	-

All information which is classified according to Dutch regulations shall be treated by the recipient in the same way as classified information of corresponding value in his own country. No part of this information will be disclosed to any party.

The classification designation Ongerubriceerd is equivalent to Unclassified.

TNO Prins Maurits Laboratory is part of
TNO Defence Research which further consists of:

TNO Physics and Electronics Laboratory
TNO Human Factors Research Institute

Netherlands Organization for
Applied Scientific Research (TNO)

Managementuittreksel

Titel	:	Trajectory Simulation Model for a Side-Thruster Guided MLRS-Type Vehicle
Auteur(s)	:	Dr. ir. G.M.H.J.L. Gadiot
Datum	:	mei 1999
Opdrachtnr.	:	A95KL410
Rapportnr.	:	PML 1998-A80

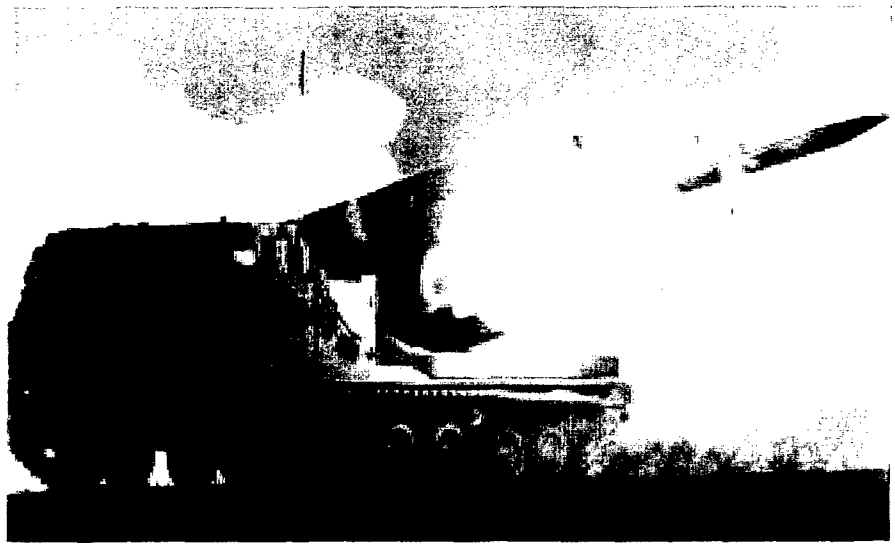

Figuur M.1: Lancering van een M26-raket vanaf een MLRS 'launcher'.

De Koninklijke Nederlandse Landmacht (KL) heeft het 'Multiple Launcher Rocket System' (MLRS) in gebruik. Met de huidige uitrusting kan men een dracht van 30+ km halen. Voor de toekomst heeft men behoefte aan een dracht van ongeveer 60 km.
Het is de doelstelling van opdracht A95KL410 om kennis en inzicht te verzamelen over MLRS-achtige systemen met een dracht van 60 km.

Ten gevolge van de grotere dracht zullen de fouten in de baan van de ongeleide raket sterker doorwerken, waardoor bij het doel grotere afwijkingen in de nauwkeurigheid optreden. De fouten worden onder andere veroorzaakt door de launcher:

- ten gevolge van zogenaamde 'tip-off' (richtingsafwijking van de raket door het contact met het lanceerplatform);
- ten gevolge van het functioneren van de voortstuwing ('thrust misalignment');
- door de invloed van de atmosfeer, onder andere de wind.

Het is mogelijk om met behulp van 'side-thrusters' de koers van de raket aan te passen en zo de raket dichter bij het doel te krijgen. In eerste instantie is onderzocht of het gebruik van side-thrusters in het zwaartepunt van de raket mogelijk is. Uit

deze studie kwam naar voren dat het mogelijk is om met behulp van 'side-thrusters' de fouten bij een range van 60 km terug te brengen naar fouten van dezelfde orde die nu optreden bij 30 km [1].

Daarna is gekeken naar de invloed van 'side-thrusters' die niet aangrijpen in het zwaartepunt van de raket. Wanneer de 'side-thrusters' aangrijpen vóór het zwaartepunt wordt het effect van de 'side-thruster'-puls versterkt. Om dit met het bestaande computermodel te evalueren is het model aangepast en is er een gedetailleerde parameterstudie uitgevoerd. De voorbereidingen en de resultaten van deze studie worden in het onderliggende rapport beschreven.

De resultaten van de studie onderschrijven de eerdere bevindingen [1] en geven aan dat ongeveer tweederde van de pulsenergie kan worden bespaard door de 'side-thrusters' zo ver mogelijk voor het zwaartepunt te plaatsen. Dit betekent dat er in principe grotere correcties mogelijk zijn of dat er met een kleinere 'thruster'module kan worden gewerkt.

[1] Gadiot, G.M.H.J.L.; Marée, A.G.M. en Keus, L.J.,
'Limited sensitivity study on side-thruster guidance for an extended range MLRS-type vehicle',
TNO-rapport PML 1997-A36, augustus 1997.

Contents

1 Introduction

This report describes the status of the work carried out by the TNO Prins Maurits Laboratory (TNO-PML) for the Royal Netherlands Army (RNlA) under project A95KL410, titled: 'Guidance concepts for indirect fire munitions' [2]. This work is related to the general interest within the military world in extending the range of artillery rocket systems. It is of particular interest to the Royal Netherlands Army who are considering upgrading their existing 30+ km range Multiple Launch Rocket System (MLRS) to a 60 km extended range version. When the range of such a ballistic rocket is upgraded, the effectiveness of these weapons will degenerate if the accuracy in position at impact is not kept at the same level or, preferably, improved. To achieve an improved accuracy, the ballistic rocket must be guided to its target. Two basic forms of guidance can be identified; aerodynamic guidance and guidance using small side-thruster rockets. This report focuses on the latter guidance method.

Within this framework, a study [1] has been performed to identify the order of the guidance effort required to realize the same target accuracy for an upgraded MLRS-like missile with a range twice as long (60 km) as currently available (30 km) and guided by side-thrusters. Furthermore, it is assumed that the guidance is performed with navigation updates sent from the ground. To prevent jamming of the signal, the guidance takes place only up to the time of apogee, for it is assumed that jamming will only occur when the missile is approaching the target, and after the missile is past its apogee. For the study, a simulation model (Direct Side Thrusting Guidance, DSTG) was developed which is able to simulate a ballistic trajectory in a standard atmosphere (US 76) of a missile from the moment the propulsion section burns out until the moment of impact. The model is based on aerodynamic data and the vehicle mass after burn-out of the propulsion section. Furthermore, a guidance algorithm is implemented with which the required side-thruster impulses can be calculated. This work is partly based on a study carried out in the US on an MLRS-type vehicle with aerodynamic guidance [3].

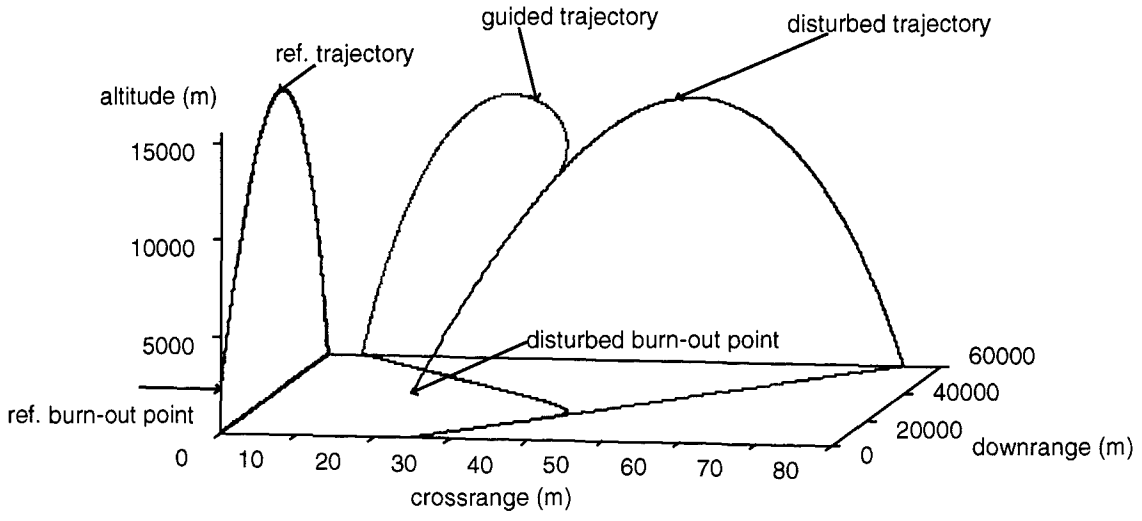

Figure 1.1: Typical reference, disturbed and side-thruster guided trajectory.

In the study, the 30 km range of an MLRS-like missile has been improved to 60 km, by increasing the velocity at burn-out. To keep the error budgets at impact for the 60 km range at the same level as for the 30 km range, the upgraded missile is guided with side-thrusters during the first half of the trajectory after burn-out up to the time of apogee. To obtain a first impression of the required guidance effort (total impulse of all side-thruster firings combined), a disturbance case with errors in the burn-out state is used as a reference. A typical reference, disturbed and side-thruster corrected trajectory is given in Figure 1.1. For determining this case, a missile with a range of 30 km and an impact just inside an assumed accuracy range of ± 50 m in cross- and downrange around the nominal ballistic point of impact was taken.
Using a linear-quadratic regulator, the upgraded MLRS-like missile could be guided such that the accuracy at impact was similar to that of the 30 km range reference vehicle. For achieving this, a total impulse of 300 - 500 Ns side-thruster firings was required.
A limited number of different guidance approaches were taken for the study, varying the total number of side-thruster firings and guidance time interval. All approaches were successful in guiding the extended range missile, but differed in the amount of total side-thruster power required.
The study showed that the greatest control effort should be applied at the beginning of the guidance time-frame. It seems to be cost effective to apply guidance as early as possible in time after burn-out.

After these initial results, the DSTG computer program was modified to include the propelled part of the guided missile flight and the influence of the weather in the form of a wind profile. The former makes it easy to introduce different propulsion

concept, e.g. the standard rocket motor or an extended range motor, and allows for a study of variations due, for example, to temperature on range and performance (typical operational aspects). The inclusion of a wind profile is important as wind effects lead to considerable deviations in missile trajectory near the target area.

In parallel, a study was carried out on the effect of side-thruster pulses that do not occur not through the centre of gravity. By taking advantage of the aerodynamic moment resulting from the side-thrust not aimed through the centre of gravity (c.o.g.), the required impulse can be diminished by up to 70%, and less total impulse is needed, or larger deviations may be corrected for.

The MLRS missile description is presented in Chapter 2. The MLRS side-thruster guidance model results with side-thrusters through the c.o.g. and with the side-thrusters not through the c.o.g. are presented in Chapters 3 and 4, respectively. An evaluation of the results is presented in Chapter 5, followed by conclusions and recommendations in Chapter 6.

2 The MLRS missile

General

The Multiple Launch Rocket System (MLRS) is a free-flight, area-fire, artillery rocket system that supplements cannon artillery fire by delivering large volumes of firepower in a short time against critical, time-sensitive targets (enemy artillery, air defence systems, mechanized units, or personnel). The MLRS provides counterbattery fire and suppression of enemy air defences, light materiel, and personnel targets. MLRS units can use their shoot and scoot capability to survive while providing up-front fire support for attacking manoeuvre elements. See Reference 1 for more detail. The MLRS consists of a self-loading launcher with an onboard fire control system (Figure 2.1). This system is mounted on a mobile track vehicle that carries twelve rockets. Each of these rockets may be fired individually or simultaneously to cover a range beyond 30 km. The basic warhead carries improved conventional submunitions. The extended range MLRS (ER-MLRS) will provide longer range rockets with lower submunition dud rates than for the MLRS. The ER-MLRS is a free-flight, area-fire, artillery rocket designed to complement the capabilities of the MLRS. Its mission is to engage targets beyond the range of the existing MLRS, up to 50 km.

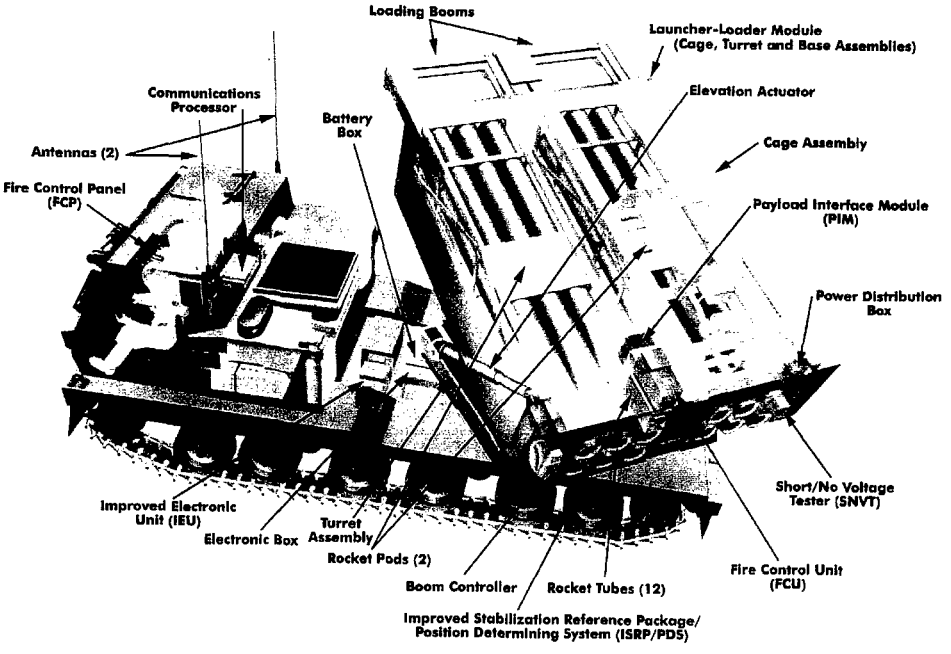

Figure 2.1: MLRS M270 missile launcher.

Performance in the Gulf War

The MLRS proved itself in the Gulf War. This was the first time the MLRS has performed in combat. During the Gulf War, the MLRS served as the 'primary counterfire weapon' against Iraqi artillery. Some of its advantages are:

- MLRS was lethal and effective against a variety of targets;
- MLRS was very manoeuverable;
- MLRS was responsive and delivered large volumes of accurate fire.

It also must be noted that the success of the MLRS is in part due to the weakness of Iraqi artillery. Nevertheless, the MLRS system proved that the future of artillery lies in a more mobile structure. Thus the MLRS has become the foundation of our future rocket launchers.

Additionally, the MLRS also had its problems during the Gulf War. In spite of the poor performance of the Iraqi artillery in the war, it is significant to note that they had (missile systems) that could outrange the MLRS. Although the range of the ATACMS is farther, it is not used as a primary counterfire weapon like the MLRS. Additionally, the MLRS faced problems in providing current meteorological data due to the extreme weather conditions. Furthermore, although many of the batteries had access to the Global Positioning System (GPS), they failed to establish an accurate known direction for laying fire. These problems were overcome due to the good training of the MLRS crew and also in part to the poor execution of Iraqi artillery.

3 MLRS side-thruster guidance model (thrusters through c.o.g.)

To simulate the ballistic flight of a missile from burn-out to impact, a computer simulation model was developed and applied. This Direct Side Thrusting Guidance (DSTG) model is based on several assumptions. In addition, some data from the literature were incorporated like, for example, the characteristics of an upgraded MLRS-like missile. In this chapter, these aspects are briefly described and discussed.

To describe the motion of a vehicle, equations of motion are required. To describe the motion of the MLRS missile the motion of a point mass is considered. The rotational dynamics, influencing the attitude of the missile, are assumed to be controlled by a passive control system (fins) so that the angle of attack of the missile is fixed at zero degrees during flight. For the description of the motion of a point mass, a three degrees of freedom model is sufficient, i.e. only the position of a point mass as a function of time. The equations of motion used are valid for the unpowered flight of a point mass over a spherical non-spinning earth at an altitude that is small with respect to the radius of the earth. The characteristics of the atmosphere are described using the US 76 Standard Atmospheric Model [5].

If disturbances occur, the trajectory of the missile will be guided by the use of side-thrusters. The firings of these side-thrusters are modelled as impulsive shots, which means that it is assumed that the time in which the firing takes place is infinitely small. As a characteristic of a side-thruster, the total impulse (Ns) is considered. The side-thruster pulses are assumed to be directed through the centre of gravity of the missile so that they only influence the direction of the trajectory and not the attitude of the missile. The interference between the side-thruster jet and the outer flowfield of the vehicle is hence neglected. Furthermore, the side-thruster impulses are directed normal to the flight velocity. The magnitude and rotational direction (of the thruster reaction force) are determined using a guidance algorithm based on a linear quadratic regulator. This algorithm is implemented in the computer simulation program using dynamic programming [3].

For the simulation of the ballistic flight of a missile, some aerodynamic, mass data and the burn-out state conditions are required. For the study in this report, the data of the MLRS-like missile presented in [3] were used. The burn-out velocity is increased by 4% in order to have a conventional downrange of 30 km. An overview of these data is given below in Table 3.1 and Figure 3.1.

Table 3.1: State of reference MLRS-like missile at burn-out.

Mass	208 kg
Velocity	803.4 m/s
Flight path angle	35°
Heading	0°
Downrange	0 m
Crossrange	0 m
Altitude	2252 m

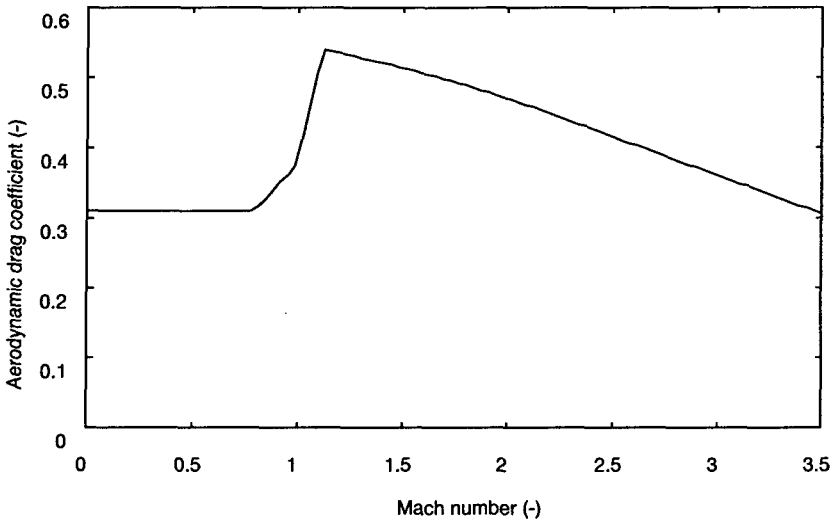

Figure 3.1: Aerodynamic drag coefficient vs. Mach number.

With the given burn-out conditions and aerodynamic drag coefficient from Figure 3.1, the resulting state conditions at impact, using the described ballistic trajectory simulation computer model, are given in Table 3.2.

Table 3.2: State of reference MLRS-like missile at impact.

Velocity	376.6 m/s
Flight path angle	-57.8°
Heading	0°
Downrange	0 m
Crossrange	30 km
Altitude	0 m

The reference MLRS-like missile with a range of 30 km is unguided. It is assumed here that the accuracy at impact of this missile lies within a range of ±50 m in cross- and downrange around the reference target. In Table 3.3 the reference and disturbed state at burn-out are presented, together with the errors in downrange and crossrange.

Table 3.3: Burn-out state error study case, downrange is 30 km.

State variable	Ref. burnout conditions	Disturbed burn-out conditions	State error at burn-out	State error at impact
Velocity (m/s)	803.4	803.6	0.2	0.2
Flight path angle (°)	35	35.045	0.045	-0.033
Heading (°)	0	0.048	0.048	0.048
Downrange (m)	0	12.5	12.5	**50.0**
Crossrange (m)	0	25.0	25.0	**50.1**
Altitude (m)	2252.5	2257.2	4.7	0

When the downrange of the MLRS is upgraded to 60 km, the target error at impact will be larger for the same errors at burn-out. The upgrade of the MLRS downrange to 60 km was achieved in this study by only increasing the flight velocity at burn-out, and keeping all other state variables the same. The state error at burn-out and at impact for this disturbed trajectory are also presented in Table 3.4.

Table 3.4: Burn-out state error study case, downrange is 60 km.

State variable	Ref. Burn-out conditions	State error at burn-out	Ref. Impact conditions	State error at impact
Velocity (m/s)	1191.7	0.2	461.8	0.5
Flight path angle (°)	35	0.045	-55.172	-0.003
Heading (°)	0	0.048	0.0	0.048
Downrange (m)	0	12.5	60000.0	**135.1**
Crossrange (m)	0	25.0	0.0	**75.2**
Altitude (m)	2252.5	4.7	0.0	0.0

From the values presented in Table 3.4, it is clear that the error in downrange and crossrange at impact are much larger for the 60 km range than for the reference range. By using side-thrusters, these errors will be reduced so that both errors will lie within the same impact accuracy range as for the reference trajectory. This will be done while at the same time the total amount of energy required for the side-thrusters is minimised.

The time interval in which guidance can be applied is from the moment of burn-out till the moment the missile reaches its apogee. After that point, it is assumed that no guidance signals can be sent to the missile anymore because of jamming. Four different cases of guidance are studied, viz.:

1 eight side-thruster firings, equally distributed in time from halfway between burn-out and apogee to apogee;
2 six side-thruster firings, equally distributed in time from halfway between burn-out and apogee to apogee;
3 ten side-thruster firings, equally distributed in time from halfway between burn-out and apogee to apogee;
4 eight side-thruster firings, equally distributed in time from burn-out to halfway between burn-out and apogee.

In Figure 3.2, the applied impulses for all four cases are presented. For the absolute values of these impulses, one is referred to Table 3.5 (see also Reference 1). From this figure it can be seen immediately that in guidance Case 4, the smallest total impulse is required, and that the maximum applied impulse is the smallest of all test cases. Furthermore, it appears that for both Cases 2 and 3, using 6 and 10 impulses respectively, the total impulse is quite similar to that of Case 1. Apparently, the total impulse for guidance is the relevant parameter to consider and not the actual number of firings.

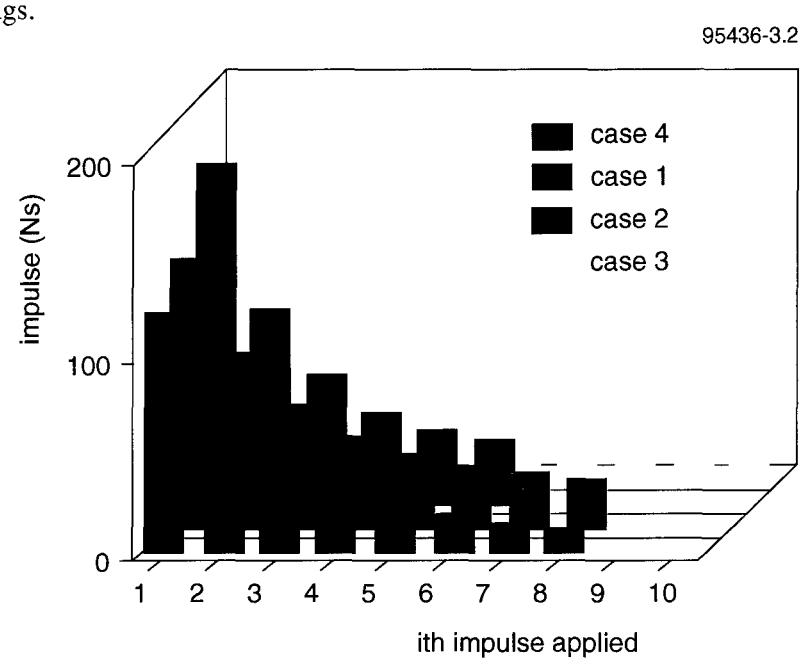

Figure 3.2: Required side-thruster impulses for the four different studied guidance cases.

Table 3.5: Required side-thruster impulses for the four different studied guidance cases.

i^{th} impulse	Case 1	Case 2	Case 3	Case 4
1	132.3	167.8	110.5	119.6
2	88.3	99.2	79.3	63.1
3	62.6	65.5	59.2	39.9
4	47.2	48.5	45.9	28.2
5	37.7	39.9	37.0	21.5
6	32.1	35.8	30.9	17.3
7	28.7	-	26.9	14.4
8	26.7	-	24.2	12.5
9	-	-	22.5	-
10	-	-	21.3	-
Total impulse (Ns)	455.7	456.6	457.9	316.4

Case 1	Guidance between halfway apogee to apogee, 8 side-thruster firings
Case 2	Guidance between halfway apogee to apogee, 6 side-thruster firings
Case 3	Guidance between halfway apogee to apogee, 10 side-thruster firings
Case 4	Guidance between burn-out to halfway apogee, 8 side-thruster firings

4 MLRS side-thruster guidance model (thrusters *not* through c.o.g.)

In the original simulation model used, it is assumed the guidance thrust is directed through the centre of mass of the vehicle, influencing only the trajectory of the missile, and not its attitude. In reality side-thrusters will in most cases influence both the trajectory and attitude of an MLRS-type vehicle. The aerodynamic forces that result from such a change in attitude can be used to help correct the trajectory of the vehicle, decreasing the necessary impulse from the side-thrusters.
Generally, to study the aspects of change in attitude, the rotational dynamics of the vehicle must be taken into account. However, using a Laplace transformation it is possible to incorporate the effects of a side-thruster firing not directed through the centre of gravity in the simulation model already developed [8]. This upgrade can then be used to perform a sensitivity study on such a side-thruster guidance system.

First the modification of the formula used to calculate the necessary impulse will be described, including the necessary positions of the centre of gravity and aerodynamic centre, and the effect of aerodynamic damping, inherent to the new impulse formula, is discussed. Then a sensitivity study is performed with the improved program, and the effect of side-thrust, not aimed through the centre of gravity, and the effect of guidance errors is discussed.

4.1 Modification of the impulse formula

The formula used by the simulation program to calculate the necessary impulse for side-thruster guidance has to be adapted in order to incorporate the effects of a change in attitude. The formula used in the original simulation was:

$$I_{tot.,orig.} = m \cdot V \cdot \sqrt{\left([\Delta\gamma]^2 + [Cos\gamma \cdot \Delta\psi]^2\right)} \qquad (4.1)$$

This formula will be derived again, but now taking into account the effect of side-thrust not directed through the vehicle's centre of mass.

4.1.1 Required impulse for $\Delta\gamma$ and $\Delta\psi$

The formula for the change of the flight path angle (for a flat, non-spinning earth, and after burn-out of the propulsion section) in time is:

$$\frac{\partial\gamma}{\partial t} = \frac{1}{m \cdot V} \cdot [\frac{1}{2} \cdot \rho \cdot V^2 \cdot S \cdot C_L - m \cdot g \cdot Cos\gamma] \qquad (4.2)$$

A side-thruster with thrust T perpendicular to the speed V will change the flight path angle, and will also induce a rotation if the thrust is not aimed through the centre of gravity. This rotation will result in a change in the aerodynamic forces on the vehicle.

The thrust is assumed constant. A Laplace transformation can be used to obtain an expression for $\gamma(s)$. By scaling the time-frame during which the side-thruster fires to $0 \le t \le \infty$, and with $\lim_{t\to\infty} \gamma(t) = \lim_{s\to 0} s \cdot \gamma(s)$, the final value of the change in flight-path angle, $\Delta\gamma$, can be calculated.
This results in:

$$\Delta\gamma = \frac{I_{tot.}}{m \cdot V} \cdot \left[1 - \frac{N_\alpha \cdot L}{M_\alpha}\right] = \frac{I_{tot.}}{m \cdot V} \cdot \left[1 - \frac{\frac{1}{2} \cdot \rho \cdot V^2 \cdot S \cdot C_{L_\alpha} \cdot L}{M_\alpha}\right] \tag{4.3}$$

In this expression, L is the distance between the side-thrusters in the nose of the vehicle and the centre of gravity, $I_{tot.}$ is the total impulse of the side-thrusters, N_α is the aerodynamic force (perpendicular to the body axes X_b and Y_b), M_α is the aerodynamic moment, $C_{L\alpha}$ is the lift coefficient as a function of the angle of attack and S is the surface area of the vehicle.
A similar expression can be obtained for the change of heading of the vehicle, induced by side-thrust.
The formula for the change of heading (for a flat, non-spinning earth, and after burn-out of the propulsion section) in time is:

$$\frac{\partial\psi}{\partial t} = \frac{1}{m \cdot V \cdot Cos\gamma} \cdot \left[\frac{1}{2} \cdot \rho \cdot V^2 \cdot S \cdot C_s\right] \tag{4.4}$$

where $C_s = C_{s_\beta} \cdot \beta = C_{L_\alpha} \cdot \beta$ if the missile is assumed to be rotational symmetrical.
Similar operations as used for the derivation of $\Delta\gamma$ result in an expression for the final value of the heading:

$$\Delta\psi = \frac{I_{tot.}}{m \cdot V \cdot Cos\gamma} \cdot \left[1 - \frac{N_\alpha \cdot L}{M_\alpha}\right] =$$
$$\frac{I_{tot.}}{m \cdot V \cdot Cos\gamma} \cdot \left[1 - \frac{\frac{1}{2} \cdot \rho \cdot V^2 \cdot S \cdot C_{L_\alpha} \cdot L}{M_\alpha}\right] \tag{4.5}$$

4.1.2 Determining the aerodynamic moment

The expressions for $\Delta\gamma$ and $\Delta\psi$ ((4.3) and (4.5), respectively) include the aerodynamic moment (as a function of α) M_α. In general, this moment can be written as [6]:

$$M_\alpha = \frac{1}{2} \cdot \rho \cdot V^2 \cdot S \cdot \bar{c} \cdot C_{M\alpha} \tag{4.6}$$

$C_{m\alpha}$ can be written as a function of the distance between a position x along the body axis and the aerodynamic centre of the missile. If the centre of gravity is taken as the position x, the resulting expression for the aerodynamic moment is:

$$M_\alpha = \frac{1}{2} \cdot \rho \cdot V^2 \cdot S \cdot C_{L_\alpha} \cdot (x_{c.g.} - x_{a.c.}) \tag{4.7}$$

4.1.3 Determining the impulse formula

Substituting (4.7) into expressions (4.3) and (4.5) results in:

$$\Delta\gamma = \frac{I_{tot.}}{m \cdot V} \cdot \left[1 - \frac{L}{(x_{c.g.} - x_{a.c.})}\right] \tag{4.8}$$

$$\Delta\psi = \frac{I_{tot.}}{m \cdot V \cdot Cos\gamma} \cdot \left[1 - \frac{L}{(x_{c.g.} - x_{a.c.})}\right] \tag{4.9}$$

Now the total value of the impulse, required to achieve $\Delta\gamma$ and $\Delta\psi$, can be calculated:

from (4.8): $$I_{tot.}(\gamma) = \frac{m \cdot V}{\left[1 - \frac{L}{(x_{c.g.} - x_{a.c.})}\right]} \cdot \Delta\gamma$$

from (4.9): $$I_{tot.}(\psi) = \frac{m \cdot V \cdot Cos\gamma}{\left[1 - \frac{L}{(x_{c.g.} - x_{a.c.})}\right]} \cdot \Delta\psi$$

and $I_{tot.} = \sqrt{\left([I_{tot.}(\gamma)]^2 + [I_{tot.}(\psi)]^2\right)}$ it follows that:

$$I_{tot.} = \frac{m \cdot V}{\left[1 - \frac{L}{(x_{c.g.} - x_{a.c.})}\right]} \cdot \sqrt{\left([\Delta\gamma]^2 + [Cos\gamma \cdot \Delta\psi]^2\right)} \tag{4.10}$$

This formula does not take into account the interference of the side-thrusters with the airflow around the vehicle, nor the shift of the aerodynamic centre or change in speed during the time of the side-thruster pulse. The formula is also only valid for small angles of attack (α and β) and does not incorporate any dampening dynamics.

4.1.4 The position of the aerodynamic centre

The position of the aerodynamic centre is not constant, but a function of the Mach number. For the reference MLRS-type vehicle (M26) used in the simulation, the following combinations of the Mach number M and $x_{c.g.}$ have been established during experiments [7].

Table 4.1: $X_{c.g.}$ versus Mach.

M	$x_{c.g.}$	M	$x_{c.g.}$	M	$x_{c.g.}$
0.4	2.815	1.2	3.003	2.5	2.504
0.8	2.844	1.4	2.974	3.0	2.300
1.0	2.840	1.6	2.915	3.5	2.129
1.1	2.958	2.0	2.731	4.0	2.040

From Table 4.1, the following graph can be produced:

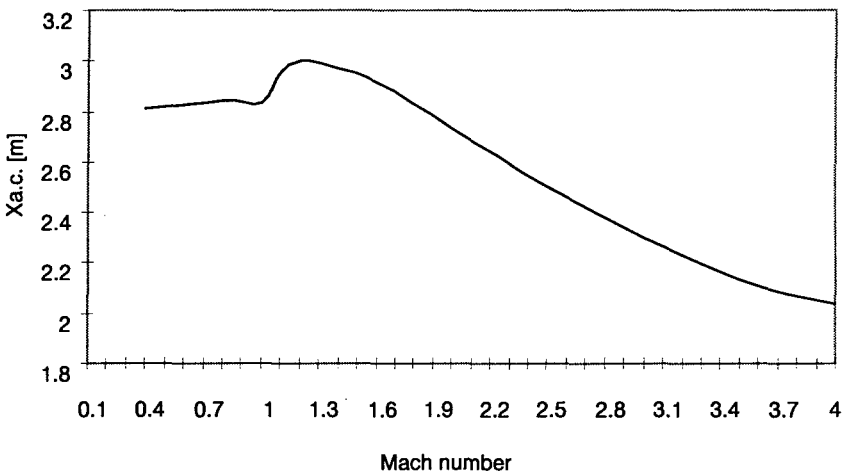

Figure 4.1: $X_{a.c.}$ versus Mach number.

In order to incorporate the position of the aerodynamic centre as a function of the Mach number, the graph above is linearised in sections, resulting in the following expressions:

$$0 \leq M \leq 1.0: \; x_{a.c.} = 0.0417 \cdot M + 2.798$$
$$1.0 < M \leq 1.1: \; x_{a.c.} = 1.180 \cdot M + 1.660$$
$$1.1 < M \leq 1.2: \; x_{a.c.} = 0.450 \cdot M + 2.463$$
$$1.2 < M \leq 1.4: \; x_{a.c.} = -0.145 \cdot M + 3.177$$
$$1.4 < M \leq 2.0: \; x_{a.c.} = -0.405 \cdot M + 3.541$$
$$2.0 < M \leq 3.0: \; x_{a.c.} = -0.431 \cdot M + 3.593$$
$$3.0 < M \leq 3.5: \; x_{a.c.} = -0.342 \cdot M + 3.326$$
$$M > 3.5: \; x_{a.c.} = -0.178 \cdot M + 2.752$$

4.1.5 The position of the centre of gravity

Because for the aerodynamic properties of the reference vehicle those of the M26 missile have been used, the M26 will also be taken as a reference for the position of the centre of gravity.
The missile consists of two parts: the propulsion section and the warhead. The mass of the propulsion section is 148.4 kg of which 97.8 kg is propellant; so after burn-out the mass of this section will be 50.6 kg. The mass of the warhead is 158 kg (the mass of the side-thrusters has not been taken into account).
The centre of gravity of the warhead has been estimated at 1.113 m from the nose, that of the propulsion section at 3.149 m. This means that the centre of gravity of the entire missile after burn-out will be approximately:

$$x_{c.g.} \approx \frac{1.113 \cdot 158 + 3.149 \cdot 50.6}{158 + 50.6} = 1.61 \text{ [m]} \qquad (4.12)$$

Figure 4.2 shows the position of this centre of gravity as well as the range of the position of the aerodynamical centre.

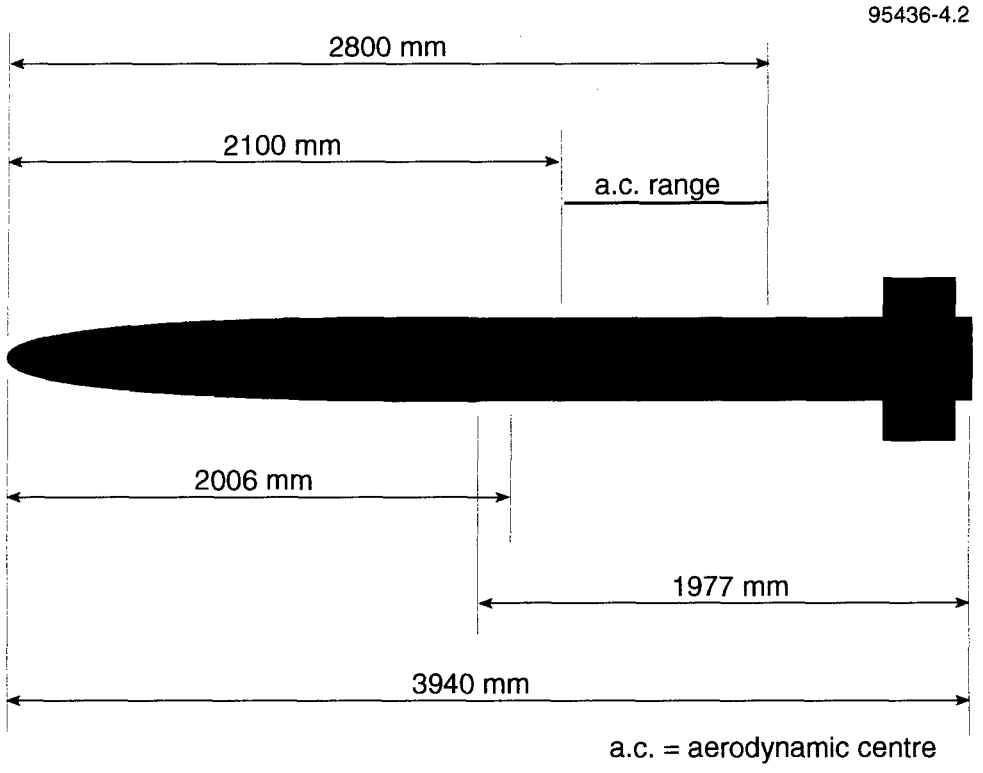

Figure 4.2: Tthe reference vehicle.

To ensure sufficient stability, the distance between the aerodynamic centre and the centre of gravity ($x_{a.c.} - x_{c.g.}$) of an unguided missile must have a certain value. Before launch ($x_{a.c.} - x_{c.g.}$) will in general have a value between one and one-and-a-half times the vehicle's diameter. The diameter of the reference vehicle is 227 mm, thus $0.227 \leq (x_{a.c.} - x_{c.g.}) \leq 0.341$ before launch.
For the situation before launch the position of the centre of gravity can be calculated.

For the situation before launch the position of the centre of gravity can be calculated. The only difference with the situation after burn-out is the centre of gravity and mass of the propellant section: 2952 mm from the nose and 148.4 kg. The position of the centre of gravity before launch will thus be approximately:

$$x_{c.g.} \approx \frac{1.113 \cdot 158 + 2.952 \cdot 148.4}{158 + 148.4} = 2.00 \text{ [m]},$$

thus, the allowed range of the aerodynamic centre is: $2.23 \leq x_{a.c.} \leq 2.34$ [m].

After burn-out the position of the centre of gravity will have changed because the propulsion section will then be empty. This position was calculated before to be 1.61 [m]. With the already established range for the aerodynamic centre, this means after burn-out: $-0.73 \leq (x_{c.g.} - x_{a.c.}) \leq -0.62$ [m] to ensure sufficient stability of the vehicle.

4.1.6 Effect of aerodynamic dampening time

To obtain formulas 4.3 (for $\Delta\gamma$) and 4.5 (for $\Delta\psi$), used to calculate the total impulse (formula 4.10), it was assumed that the duration of the side-thruster pulse is negligible. Changes in γ and ψ induced by side-thrust are assumed to be instant, because the duration of a side-thruster pulse is small compared to the total flight time.

When a side-thrust impulse starts rotating the vehicle, the resulting aerodynamic moment will try to increase the flight angle and/or heading. This moment is counteracted by the moment which results from the stability of the vehicle. It will take time before these two moments are in balance and the rotation is dampened out.
This time is neglected in the simulation program, as it is assumed to be short. To verify if this assumption is correct, an inverse Laplace transform of:

$$\gamma(s) = \frac{1}{s^2} \cdot \frac{T}{m \cdot V} \cdot \frac{\left[\frac{N_\alpha \cdot L}{I_{yy}} + \frac{N_\alpha \dot{\theta}(0) \cdot s}{T} + s^2 - \frac{M_\alpha}{I_{yy}} \right]}{\left[s^2 - \frac{M_\alpha}{I_{yy}} + \frac{s \cdot N_\alpha}{m \cdot V} \right]} \tag{4.13}$$

and 1.16:

$$\psi(s) = \frac{1}{s^2} \cdot \frac{T}{m \cdot V \cdot Cos\gamma} \cdot \frac{\left[\frac{N_\alpha \cdot L}{I_{yy}} + \frac{N_\alpha \dot{\chi}(0) \cdot s}{T} + s^2 - \frac{M_\alpha}{I_{yy}} \right]}{\left[s^2 - \frac{M_\alpha}{I_{yy}} + \frac{s \cdot N_\alpha}{m \cdot V \cdot Cos\gamma} \right]} \tag{4.14}$$

should be obtained to find γ and ψ as a function of time.
The variables in both formulas change in time, but because the duration of a side-thruster pulse is very short, and to obtain expressions for γ and ψ which are only dependent on the thrust T and the pulse duration, all other variables are assumed to be constant for the duration of the pulse.

When the values of γ and ψ [1] for a certain control time-point are compared for cases with and without guidance, it can be concluded that for a certain side-thruster pulse, the required $\Delta\gamma$ is in the order of 0.1 degrees and the required $\Delta\psi$ is in the order of 0.02 degrees. The required $\Delta\gamma$ is thus the dominating factor in the total required angle change. Furthermore, the expressions for $\gamma(s)$ and $\psi(s)$ are almost the same, except for the cos γ term (which is about 1 during the guidance interval). Therefore, only the expression for $\Delta\gamma$ will be studied from here on.

A side-thruster pulse early in the flight, for the moment when V = 940 m/s, is taken as a typical case. At this moment, the variables in formulas 4.13 and 4.14 (except T) are:

- V = 940 m/s
- m = 207.97 kg
- L = 1.60 (maximum value for L)
- M = 3
- h = 7290 m
- $\rho = 0.5696$ kg/m^3
- $x_{c.g.} = 1.61$ m
- $x_{a.c.} = 2.30$ m
- $C_{N\alpha} = 6.77$
- d = 0.227
- l = 3.940

Furthermore, it is assumed that $\theta(0)$ is zero, and T is constant.

If the above values are used to calculate the variables in the formula for $\gamma(s)$, the inverse Laplace transformation results in:

$$\gamma(t) =$$

$$T \cdot \left[-2.79 \cdot 10^{-8} + 1.69 \cdot 10^{-5} \cdot t + e^{-12.25 \cdot t} \cdot \left(2.79 \cdot 10^{-8} \cdot \cos(121 \cdot t) - 9.44 \cdot 10^{-8} \cdot \sin(121 \cdot t) \right) \right]$$

In the original program this was: $\gamma(t)_{original} = \dfrac{T \cdot t}{m \cdot V} = \dfrac{T \cdot t}{1.95 \cdot 10^5}$

For T=300 N, $\gamma(t)$ is plotted in Figure 4.3 for the original and for the upgraded simulation program.

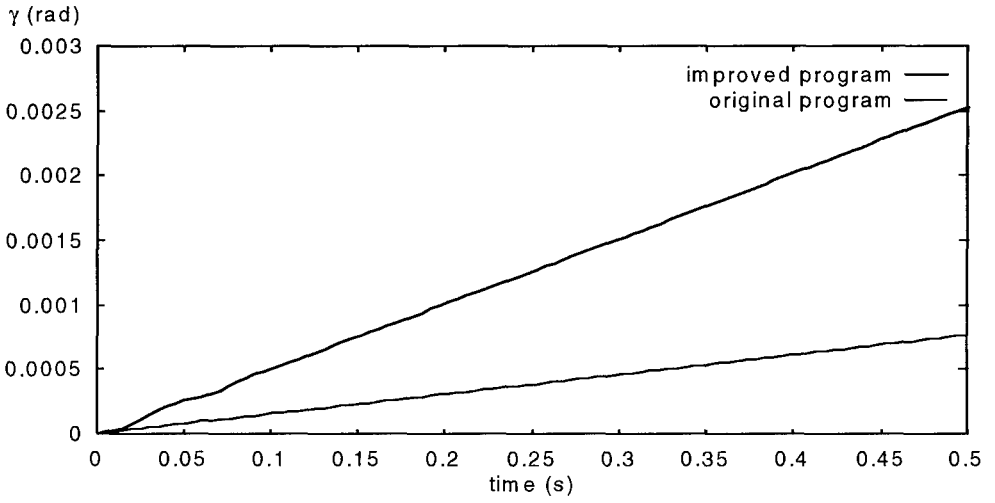

Figure 4.3: $\gamma(t)$ for T = 300 N, for guidance point t ≈ 7.4 s, V = 940 m/s, h = 7.3 km and, L = 1.60 m, plotted for the original and the improved program.

From Figure 4.3, it is clear that a certain γ is reached earlier according to the upgraded program than according to the original program. The aerodynamic forces, resulting from side-thrust which is not aimed through the centre of gravity of the vehicle, clearly help change the flight angle.

To study the influence of the aerodynamic forces which are introduced in the upgraded program, $\gamma(t)/\gamma(t)_{original}$ (which is not a function of T) can be plotted, as in Figure 4.4.

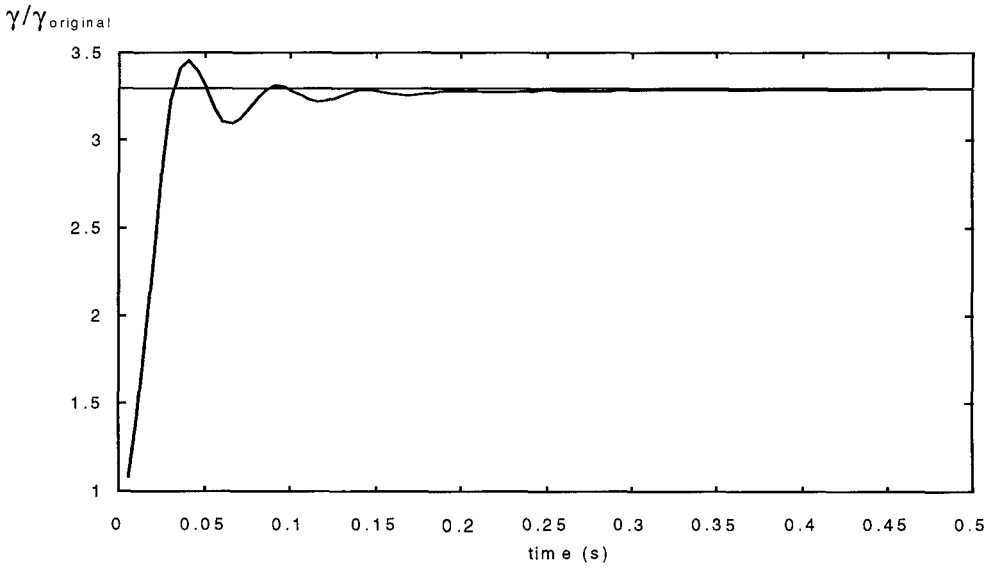

Figure 4.4: $\gamma/\gamma_{original}$ as a function of time for guidance point t ≈ 7.4 s, V = 940 m/s, h = 7.3 km and L = 1.60 m.

The horizontal line in the figure represents the end value $\Delta\gamma/\Delta\gamma_{original}$, which can be calculated by dividing $\Delta\gamma$ (Formula 4.3) by $\Delta\gamma_{original} = I_{tot.}/m \cdot V$ (which is the expression for $\Delta\gamma$ used in the original simulation program):

$$\frac{\Delta\gamma}{\Delta\gamma_{original}} = \frac{\frac{I_{tot.}}{m \cdot V} \cdot \left[1 - \frac{N_\alpha \cdot L}{M_\alpha}\right]}{\frac{I_{tot.}}{m \cdot V}} = 1 - \frac{N_\alpha \cdot L}{M_\alpha} = 1 + \frac{L}{(x_{a.c.} - x_{c.g.})} \qquad (4.16)$$

In Figure 4.4, it can be seen that $\gamma/\gamma_{original}$ includes a dampening effect because of the introduced aerodynamics. The graph starts at 1 for t = 0, because then $\gamma = \gamma_{original}$. The end value of 3.3 shows that for the same impulse, $\Delta\gamma$ is 3.3 times larger if L = 1.60 instead of L = 0 (as was the case in the original program). In this case, the oscillation is damped out after about 0.2 seconds. This is short compared to the total flight time of about 110 seconds, so the assumption of an instant angle change still holds when the side-thrust is not aimed through the centre of gravity. If the time between two guidance intervals (and when $V \approx 940$ m/s) is in the order of 0.2 seconds or less however, the dampening time cannot be neglected anymore. During the time when the missile can be guided, the variables such as speed, air density etc. change, which will have an effect on $\gamma(t)/\gamma(t)_{original}$. To study this effect, $\gamma(t)/\gamma(t)_{original}$ can be plotted for various guidance time points between burn-out and apogee. Figures 4.5 to 4.10 show $\gamma/\gamma_{original}$ as a function of time for various guidance points.

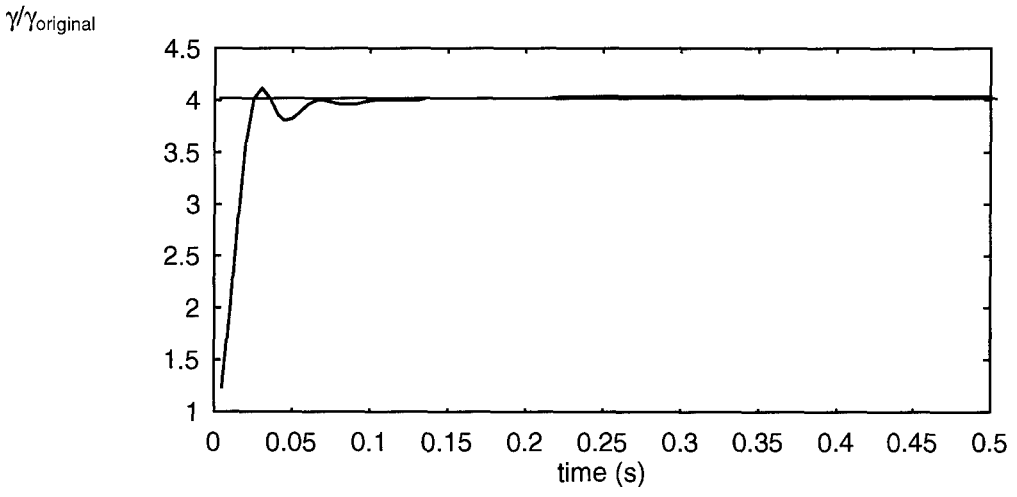

Figure 4.5 *$\gamma_{original}$ as a function of time for guidance point t ≈ 0.0 s, V = 1192 m/s, h = 2.3 km and L = 1.60 m.*

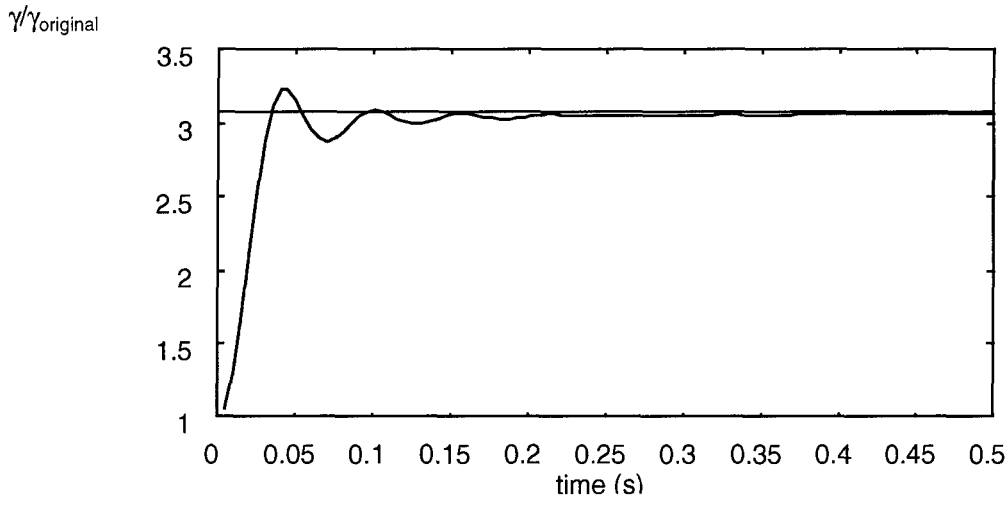

Figure 4.6: $\gamma/\gamma_{original}$ *as a function of time for guidance point* $t \approx 10.6$ *s,* $V \approx 872$ *m/s,* $h = 8.0$ *km and* $L = 1.60$ *m.*

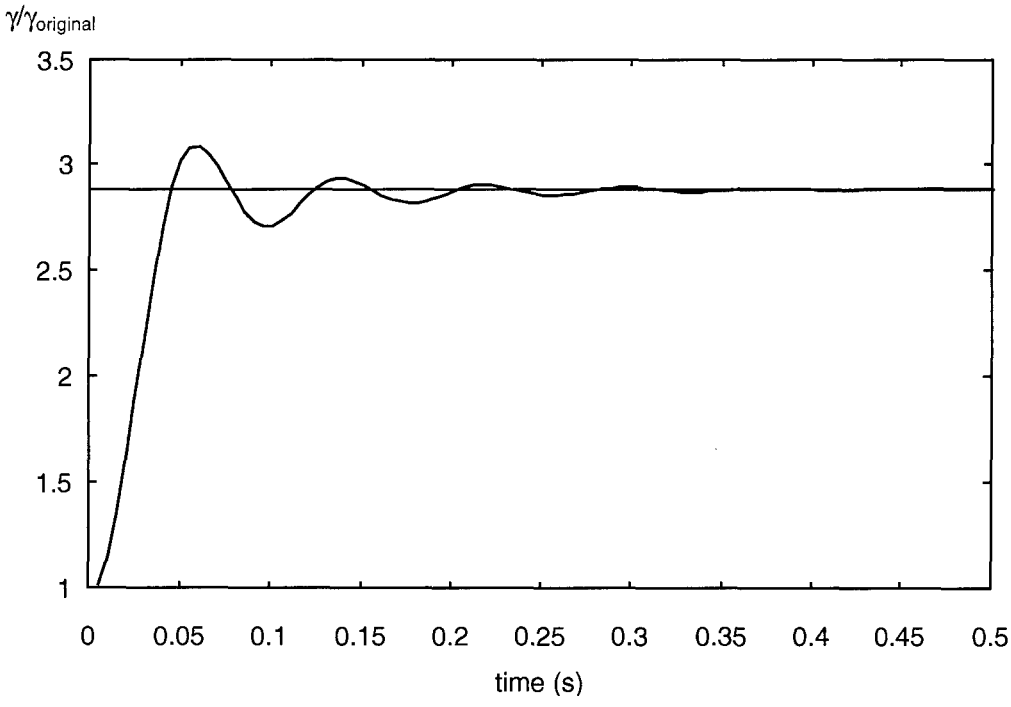

Figure 4.7: $\gamma/\gamma_{original}$ *as a function of time for guidance point* $t \approx 21.1$ *s,* $V = 717$ *m/s,* $h = 11.8$ *km and* $L = 1.60$ *m.*

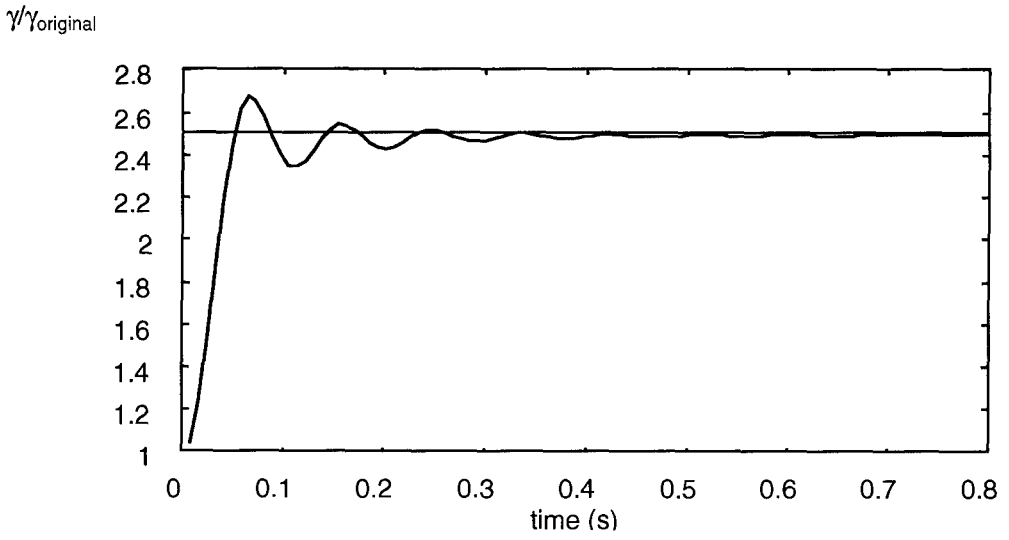

Figure 4.8: $\gamma/\gamma_{original}$ *as a function of time for guidance point* $t \approx 31.7$ *s,* $V = 629$ *m/s,* $h = 14.7$ *km and* $L = 1.60$ *m,*

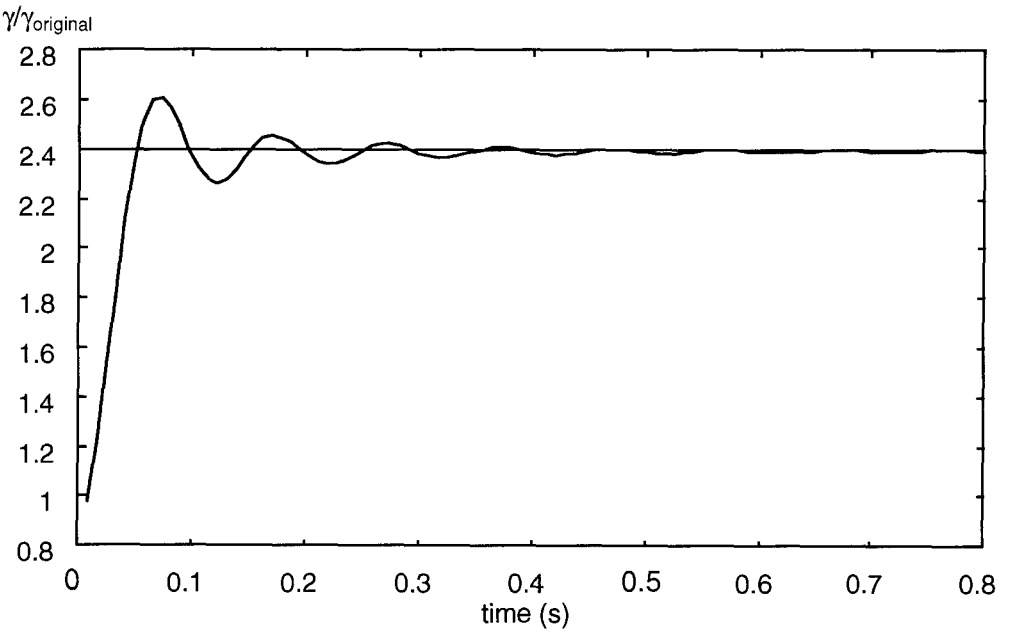

Figure 4.9: $\gamma/\gamma_{original}$ *as a function of time for guidance point* $t \approx 42.2$ *s,* $V = 576$ *m/s,* $h = 15.3$ *km and* $L = 1.60$ *m.*

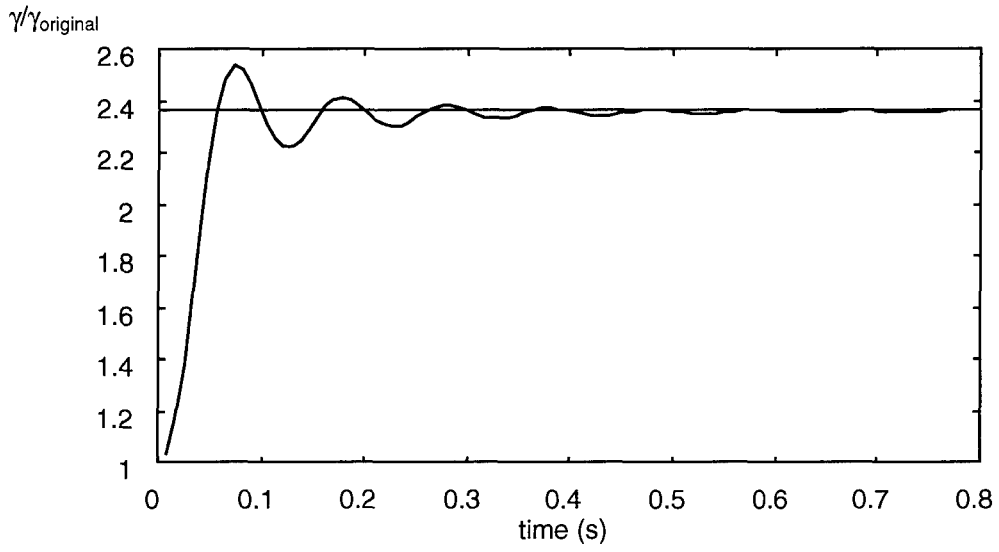

Figure 4.10: $\gamma/\gamma_{original}$ as a function of time for guidance point t ≈ 47.75 s, V = 558 m/s, h = 15.5 km and L = 1.60 m.

The graphs show that $\Delta\gamma/\Delta\gamma_{original}$ decreases for later guidance points, which means the advantage of side-thrust not aimed through the centre of gravity decreases for later guidance points. This is clear from expression 4.10; L and $x_{c.g.}$ are constant, but $x_{a.c.}$ increases in time, thus increasing $(x_{a.c.}-x_{c.g.})$.
It is also clear that the damping time increases for later guidance points. For guidance at t = 0.0 s the final value of $\Delta\gamma/\Delta\gamma_{original}$ is obtained after about 0.15 seconds. For t = 21.1 s, this is 0.30 seconds, and for t = 47.75 s, it is about 0.60 seconds. The dampening time at the last guidance points (when the missile has almost reached its apogee) is still short, and so should not have a significant effect on the vehicle's trajectory. The dampening time should, however, be taken into consideration when the time between subsequent guidance points is determined.

Above considerations indicate that for a first impression of the dynamics of side-thruster guidance, the simulation program without dampening time should be adequate.

4.2 Sensitivity study

In the following, several sensitivity analyses will be performed the ammount of guidance effort needed, using side-thrusters, to drive the error at impact for the upgraded MLRS within the ±50 m in downrange and crossrange if the range of the missile is extended from 30 km to 60 km will be examined for each case.
The upgrading of the MLRS downrange to 60 km is achieved in this simulation by increasing the flight velocity at burn-out while keeping all other state variables the same. The influence of the extra boost on the mass at burn-out is neglected.

4.2.1 First analysis of the influence of L on the required impulse

Without running the upgraded simulation program, already a lot can be learned from studying the formula used to calculate the required impulses. In the original program this was:

$$I_{tot.,orig.} = m \cdot V \cdot \sqrt{\left(\left[\Delta\gamma\right]^2 + \left[Cos\gamma \cdot \Delta\psi\right]^2\right)} \qquad (4.1)$$

In the upgraded program this formula is:

$$I_{tot.} = \frac{m \cdot V}{\left[1 - \frac{L}{(x_{c.g.} - x_{a.c.})}\right]} \cdot \sqrt{\left(\left[\Delta\gamma\right]^2 + \left[Cos\gamma \cdot \Delta\psi\right]^2\right)} \qquad (4.10)$$

Formula (4.10) is very similar to (4.1), except for the term: $\left[1 - L/(x_{c.g.} - x_{a.c.})\right]$.

This means (4.1) is a limit case of (4.10) when L = 0, corresponding with side-thrusters directed through the centre of gravity.

For a stable vehicle, the aerodynamic centre must be positioned behind the centre of gravity, which means ($x_{c.g.}$ - $x_{a.c.}$) will be negative, and therefore $\left[1 - L/(x_{c.g.} - x_{a.c.})\right] \geq 1$.

This means if $L \neq 0$, the required impulse will be lower than calculated with formula (4.1).

Indeed, for the reference vehicle used in the simulation, ($x_{c.g.}$ - $x_{a.c.}$) is negative throughout the entire flight, so the aerodynamic forces on the missile can be used to guide the vehicle with less effort from the side-thrusters.

To estimate how much the aerodynamic forces (which result from side-thrust not aimed through the centre of gravity) can reduce the required impulse, an average position of the aerodynamic centre for the guidance time interval can be applied. If the guidance is applied between burn-out and halfway to the apogee (t = 23.75 s.), then the time halfway in the guidance interval is t = 11.85 s, where according to the simulation program the Mach number is 2.77. For M = 2.77 the position of the aerodynamic centre can be deduced from Figure 1.01: $x_{a.c.}$= 2.4 m.

If the maximum possible distance for the side-thrusters (limited by the length of the reference vehicle) is applied, then L = 1.60 m. This means (with $x_{c.g.}$= 1.61 m):

$\left[1 - L/(x_{c.g.} - x_{a.c.})\right]$ = 1 - 1.60/(1.61 - 2.4) = 3.0 $\Rightarrow$

$$I_{tot.} = \frac{m \cdot V}{\left[1 - \frac{L}{(x_{c.g.} - x_{a.c.})}\right]} \cdot \sqrt{\left(\left[\Delta\gamma\right]^2 + \left[Cos\gamma \cdot \Delta\psi\right]^2\right)} =$$

$$\frac{1}{3.0} \cdot m \cdot V \cdot \sqrt{\left(\left[\Delta\gamma\right]^2 + \left[Cos\gamma \cdot \Delta\psi\right]^2\right)} = 0.33 \cdot I_{tot.,orig.}$$

This means a required impulse given at t = 11.85 can be reduced with as much as 67% if the side-thrust is not aimed through the centre of gravity of the vehicle.

From formulas (4.1) and (4.10) it is clear that:

$$I_{tot.}/\, I_{tot.,orig.} = \frac{1}{\left[1 - \frac{L}{(x_{c.g.} - x_{a.c.})}\right]} \qquad (4.17)$$

The reduction in the required impulse, i.e. $(1 - I_{tot.}/ I_{tot.,orig.})$, is a function of L and $(x_{c.g.} - x_{a.c})$.
In the time interval which can be used for guidance (between burn-out and apogee) $x_{a.c.}$ varies between 2.11 and 2.78. Assuming a margin of 30% on the estimated position of the centre of gravity, $x_{c.g.}$ can vary from 1.13 to 2.09. This means the value of $(x_{c.g.} - x_{a.c})$ can vary between -1.65 and -0.02. L can be varied between 0 and 1.60.

In Table 4.2 and Figure 4.11,the influence of L and $(x_{c.g.} - x_{a.c})$ on the reduction in the required impulse $(1 - I_{tot.}/ I_{tot.,orig.})$ is shown.

Table 4.2: $(1 - I_{tot.}/ I_{tot.,orig.})$ as a function of L and $(x_{c.g.} - x_{a.c})$.

$(x_{c.g.} - x_{a.c})$ [m]:	-0.02	-0.35	-0.67	-1.00	-1.32	-1.65
L [m]:						
0	0%	0%	0%	0%	0%	0%
0.04	67%	10%	6%	4%	3%	2%
0.08	80%	19%	10%	7%	6%	5%
0.32	94%	48%	32%	25%	20%	16%
0.64	97%	65%	49%	39%	33%	28%
0.96	98%	73%	59%	49%	42%	37%
1.28	98%	79%	66%	56%	49%	44%
1.60	99%	82%	70%	62%	55%	49%

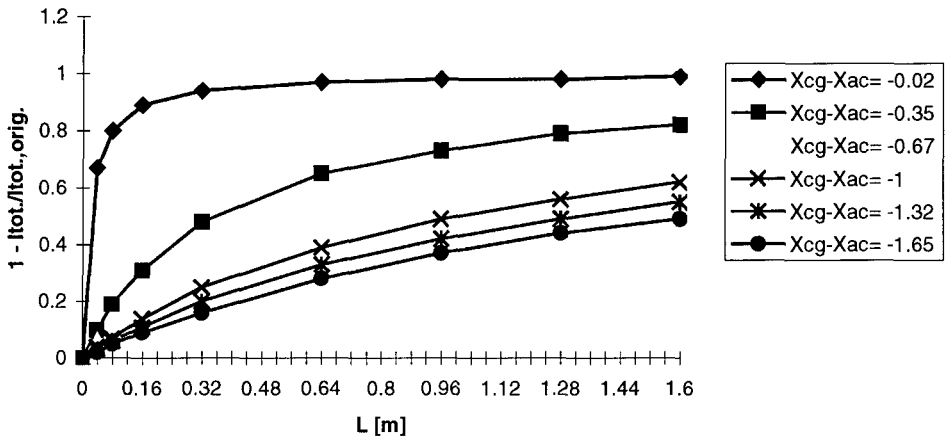

Figure 4.11: (1 - $I_{tot.}$/ $I_{tot.,orig.}$) for different values of ($x_{c.g.}$ - $x_{a.c}$), as a function of L.

From the table and the figure it is clear that the reducing effect of ($x_{c.g.}$ - $x_{a.c}$) on the required impulse increases for higher values of L. Also the amount of reduction increases faster for smaller values of ($x_{c.g.}$ - $x_{a.c}$).

As ($x_{c.g.}$ - $x_{a.c}$) approaches zero,the reduction in required impulse approaches 100%.
In reality the distance between the centre of gravity and the aerodynamic centre will have a minimum greater than zeroto insure the stability of the missile. For sufficient stability, the value of ($x_{c.g.}$ - $x_{a.c}$) must be: $-0.73 \leq (x_{c.g.} - x_{a.c}) \leq -0.62$.
From Figure 4.11, it can therefore be concluded that for a stable missile, the possible reduction in total impulse will be approximately 0 to 70%.

4.2.2 Simulation ozf previous cases

To study the effect of side-thrust not aimed through the centre of gravity, the cases evaluated in Chapter 3 will be studied again. In Chapter 3, only launch-induced offsets at burn-out were taken into account. For a 30 km reference trajectory of the missile, a disturbed case, with errors for all state variables at burn-out, was selected for which the MLRS impacts just at the border of its assumed ±50 m accuracy range. All state variables contribute equally to the error in downrange and crossrange at impact. Table 4.3 presents the reference and disturbed state at burn-out, together with the errors in downrange and crossrange.

Table 4.3: Burn-out state error study case, downrange = 30 km.

State variable	Ref. burn-out conditions	Disturbed burn-out conditions	State error at burn-out	State error at impact
Velocity (m/s)	803.4	803.6	0.2	0.2
Flight path angle (°)	35	35.045	0.045	-0.033
Heading (°)	0	0.048	0.048	0.048
Downrange (m)	0	12.5	12.5	**50.0**
Crossrange (m)	0	25.0	25.0	**50.1**
Altitude (m)	2252.5	2257.2	4.7	0

Four different cases of guidance were studied, varying the number of side-thruster pulses and the guidance time frame:

1 eight side-thruster pulses, equally distributed in time from halfway between burn-out and apogee to apogee (L = 0);
2 six side-thruster pulses, equally distributed in time from halfway between burn-out and apogee to apogee (L = 0);
3 ten side-thruster pulses, equally distributed in time from halfway between burn-out and apogee to apogee (L = 0);
4 eight side-thruster pulses, equally distributed in time from burn-out to halfway between burn-out and apogee (L = 0).

The results of this study are presented in Table 4.4.

Table 4.4: Required side-thruster impulses (Ns).

i^{th} impulses	Case 1	Case 2	Case 3	Case 4
1	132.3	167.8	110.5	119.6
2	88.3	99.2	79.3	63.1
3	62.6	65.5	59.2	39.9
4	47.2	48.5	45.9	28.2
5	37.7	39.9	37.0	21.5
6	32.1	35.8	30.9	17.3
7	28.7		26.9	14.4
8	26.7		24.2	12.5
9			22.5	
10			21.3	
Total impulse (Ns)	455.7	456.6	457.9	316.4

As already concluded in Chapter 3, the total impulse for Case 4 is lower than for the other three, because the error in the trajectory will grow in time. Therefore the sooner this error is compensated, the better. Case 4 involves guidance right after burn-out; for the other cases guidance only takes place from halfway burn-out.

When using the upgraded simulation program to recalculate these four cases, with the distance between the centre of gravity and the side-thrusters L = 1.60 m and $x_{c.g.}$ = 1.61 m, the following results are found.

Table 4.5: Required side-thruster impulses (Ns) for the four different studied guidance cases, using the upgraded simulation program with L = 1.60 m.

i^{th} impulses	Case 1	Case 2	Case 3	Case 4
1	50.1	63.5	41.8	26.0
2	34.2	38.7	30.6	16.0
3	24.7	26.2	23.2	11.2
4	18.9	19.7	18.3	8.6
5	15.4	16.5	14.9	6.9
6	13.2	14.9	12.6	5.8
7	11.9		11.1	5.0
8	11.2		10.0	4.4
9			9.4	
10			8.9	
Total impulse (Ns)	179.6	179.5	180.8	83.8

The impulses calculated with the new simulation program are significantly lower than those calculated with the original program, as was expected. For Cases 1 to 3, a reduction of 60 – 61% was achieved, while Case 4 was reduced by 73.5%. The number of side-thruster pulses does not seem to be important for the amount of required impulse.
For Case 4, the reduction is significantly higher than for the other cases. This is because of the additional impulse reducing effect of the most optimal value for $x_{a.c.}$ at burn-out. Guidance in the time-interval between burn-out and halfway apogee becomes even more cost-effective when the side-thrust is not aimed through the centre of gravity.

4.2.3 Simulation of additional cases

According to Chapter 3, the number of pulses of the side-thrusters system is not important, but only a very limited number of cases have been studied. To investigate the influence of the number of pulses in more detail, additional cases were studied, varying the number of pulses and assuming the same launch-induced offsets at burn-out as in Cases 1 to 4.
Guidance is indicated to be most effective at the beginning of the guidance time-frame. This would indicate that the best time to fire the side-thrusters is right after burn-out (t = 0). Also right after burn-out the position of $x_{a.c.}$ is the most optimal, which means a lower impulse for a given set of angle changes.
However, V is maximal at t = 0, which has an increasing effect on the required impulse. There must be an optimal moment or time-frame after burn-out to use the side-thrusters. This moment is not dependent on $x_{c.g.}$ or L, only on the required angle change ($\Delta\gamma$, $\Delta\psi$), the position of the aerodynamic centre and speed V, so $x_{c.g.}$ and L will not be varied.
The following cases involve variation of the time-frame of thruster burn in the considered guidance time interval (t = 0 till apogee at t = 47.50 sec.) and variation of the number of pulses, while $x_{c.g.}$ and L are kept constant (nominal $x_{c.g.}$ = 1.61 m and maximal L = 1.60 m).

5 guidance between burn-out (t = 0) and halfway apogee (t = 23.75 s), 10 side-thruster pulses.
6 guidance between burn-out (t = 0) and halfway apogee (t = 23.75 s), 6 side-thruster pulses.
7 guidance between burn-out (t = 0) and halfway apogee (t = 23.75 s), 4 side-thruster pulses.
8 guidance between burn-out (t = 0) and halfway apogee (t = 23.75 s), 2 side-thruster pulses.
9 guidance between burn-out (t = 0) and quarter-way apogee (t = 11.88 s), 10 side-thruster pulses.
10 guidance between burn-out (t = 0) and quarter-way apogee (t = 11.88 s), 8 side-thruster pulses.
11 guidance between burn-out (t = 0) and quarter-way apogee (t = 11.88 s), 6 side-thruster pulses.
12 guidance between burn-out (t = 0) and quarter-way apogee (t = 11.88 s), 4 side-thruster pulses.
13 guidance between burn-out (t = 0) and quarter-way apogee (t = 11.88 s), 2 side-thruster pulses.

Tables 4.6 and 4.7 and Figures 4.12 and 4.13 show the results for these cases (and Case 4):

Table 4.6: Required side-thruster impulses (Ns) for Case 5 to 8 and Case 4.

i^{th} impulse	Case 5	Case 4	Case 6	Case 7	Case 8
1	22.0	26.0	31.3	40.2	54.7
2	14.6	16.0	17.2	18.3	19.0
3	10.7	11.2	11.6	11.8	
4	8.3	8.6	8.7	8.8	
5	6.8	6.9	6.9		
6	5.7	5.8	5.9		
7	4.9	5.0			
8	4.3	4.4			
9	3.9				
10	3.6				
Total Impulse (Ns)	84.9	83.8	81.6	79.2	73.7

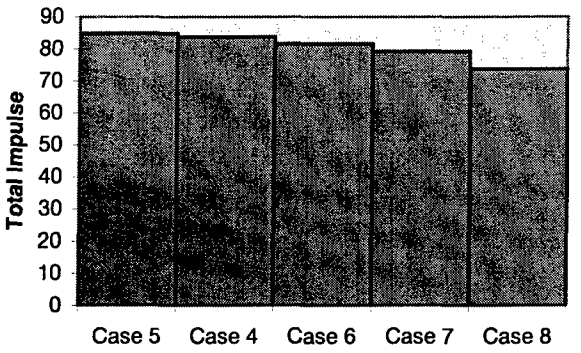

Figure 4.12: The total impulse of Cases 4 to 8.

Table 4.7: Required side-thruster impulses (Ns) for Cases 9 to 13.

i^{th} impulse	Case 9	Case 10	Case 11	Case 12	Case 13
1	24.8	30.2	37.8	50.5	73.7
2	16.7	18.5	20.1	20.7	17.6
3	12.3	12.8	13.0	12.7	
4	9.5	9.5	9.5	9.4	
5	7.6	7.6	7.6		
6	6.4	6.3	6.4		
7	5.4	5.4			
8	4.8	4.8			
9	4.3				
10	3.9				
Total Impulse (Ns)	95.7	95.1	94.3	93.3	91.3

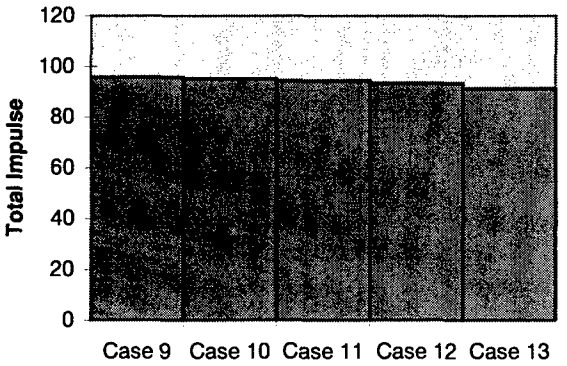

Figure 4.13: The total impulse of Cases 9 to 13.

The results show that the largest impulses are applied at the start of each chosen case. This was expected because the induced errors at burn-out will grow in time,

and thus the cost to correct them will also increase in time. This conclusion is the same as stated in Chapter 3.

It can also be observed that the required total impulse increases for higher numbers of side-thruster burns. This can also be explained by the growth of the errors in time; the lower the number of side-thruster burns, the higher the first impulse at $t = 0$ (see Tables 4.6 and 4.7) and thus the more effective the error is compensated.

Furthermore, it can be seen that the required total impulses for the cases with guidance till halfway burn-out are lower than those for the cases with guidance till quarter-way burn-out. Especially, the first impulse at $t = 0$ (see Tables 4.6 and 4.7) for guidance till halfway burn-out is much lower than for guidance till quarter-way burn-out (for equal numbers of thruster burns). This is because all the guidance has to be performed shortly after burn-out for guidance till quarter-way burn-out The speed is then maximal, which has an increasing effect on the required impulse (outweighing the decreasing effect of the more optimal position of the aerodynamic centre).

In the previous cases, guidance between burn-out and apogee was not considered. To complement the results, the following case was studied:

14 guidance between burn-out ($t = 0$) and apogee ($t = 11.88$ s), two side-thruster pulses.

The results of Case 14 are presented in the following table.

Table 4.8: Required side-thruster impulses (Ns) for Case 14.

i^{th} impulse	Case 14
1	58.7
2	22.1
Total Impulse (Ns)	80.8

The required total impulse for Case 14 is 80.8 Ns, which is more than for Case 8, but less than for Case 13. The optimum guidance interval is thus between burn-out ($t = 0$) and halfway apogee ($t = 23.75$ s).

4.2.4 Effect of guidance errors on the required impulse

In the simulation program, the disturbed trajectory of the missile is compared with the desired reference trajectory. By this comparison the errors in the trajectory can be calculated, and therefore the necessary $\Delta\gamma$ and $\Delta\psi$ at each control point to correct the trajectory (the required impulse is calculated as a function of $\Delta\gamma$ and $\Delta\psi$ afterwards, and has no direct influence on the trajectory). Subsequently, the new (corrected) values for γ and ψ are calculated by adding $\Delta\gamma$ and $\Delta\psi$:

$$\gamma = \gamma + \Delta\gamma$$
$$\psi = \psi + \Delta\psi$$

In reality, the command post from where the MLRS-type vehicle is launched will track the missile's trajectory, and subsequently transmit the required side-thruster impulses to correct it. The required impulses will be calculated using the known characteristics of the missile.
If however the characteristics of the launched missile are not the same as those of the reference missile (which is used to calculate the desired reference trajectory), the calculated guidance impulses will not be correct. The incorrect impulses will introduce errors in the trajectory which, subsequently, will also have to be compensated. The resulting total impulse that is required from the side-thrusters will thus change.

In reality the guidance errors will result from differing characteristics of the real vehicle when compared to the reference vehicle. When for instance the propellant is not burned away completely after burn-out, the centre of gravity can differ from that calculated, or the outer surface of the missile might be damaged, changing the aerodynamic characteristics.
The simulation program calculates the trajectories for a point mass, so the positions of the centre of gravity and the aerodynamic centre are not included in the calculations, and rotations of the vehicle do not influence the trajectory. The effects of differing aerodynamic characteristics and errors in the positions of the aerodynamic centre and the centre of gravity are thus not easy to incorporate in the program.

The simplest way to introduce guidance errors in the simulation program is to include errors in the calculated values for γ and ψ after each guidance effort. In this way the effects of a whole range of possible errors in the vehicle's characteristics can be covered:

$$\gamma = \gamma + \Delta\gamma + \gamma_{error}$$
$$\psi = \psi + \Delta\psi + \psi_{error}$$

(The required impulse is of course only a function of $\Delta\gamma$ and $\Delta\psi$ and not of γ_{error} and ψ_{error}; the errors only effect the guided trajectory after each control point, not the required angle changes at the control points themselves.)
The errors in γ and ψ caused by different characteristics of the missile will be assumed to be percentages of $\Delta\gamma$ and $\Delta\psi$, thus if the guidance error factor is X:

$$\gamma = \gamma + \Delta\gamma + X\cdot\Delta\gamma = \gamma + (1+X)\cdot\Delta\gamma$$
$$\psi = \psi + \Delta\psi + X\cdot\Delta\psi = \psi + (1+X)\cdot\Delta\psi$$

Effect of guidance errors as a function of the number of guidance pulses
To study the influence of γ_{error} and ψ_{error} on the required impulse as a function of the number of guidance pulses, the following cases are performed and compared (for all cases L = 1.60 m and $x_{c.g.}$ = 1.61 m; the burn-out error is the same as presented in Table 4.3):

Cases with guidance between burn-out (t = 0) and halfway apogee (t = 23.75 s), ten thruster pulses

- Case 5A: X = -10%
- Case 5B: X = -5%
- Case 5 : X = 0
- Case 5C: X = 5%
- Case 5D: X = 10%

Cases with guidance between burn-out (t = 0) and halfway apogee (t = 23.75 s), six thruster pulses

- Case 6A: X = -10%
- Case 6B: X = - 5%
- Case 6 : X = 0
- Case 6C: X = 5%
- Case 6D: X = 10%

Cases with guidance between burn-out (t = 0) and halfway apogee (t = 23.75 s), two thruster pulses

- Case 8A: X = -10%
- Case 8B: X = -5%
- Case 8 : X = 0
- Case 8C: X = 5%
- Case 8D: X = 10%

The results of these cases are presented in the following tables and figures.

Table 4.9: Required side-thruster impulses (Ns) for Cases 5 to 5D.

i^{th} impulse	Case 5A	Case 5B	Case 5	Case 5C	Case 5D
1	22.0	22.0	22.0	22.0	22.0
2	15.1	14.9	14.6	14.4	14.1
3	11.3	11.0	10.7	10.4	10.1
4	8.9	8.6	8.3	8.0	7.8
5	7.3	7.0	6.8	6.6	6.3
6	6.1	5.9	5.7	5.5	5.3
7	5.3	5.1	4.9	4.8	4.6
8	4.6	4.5	4.3	4.2	4.0
9	4.1	4.0	3.9	3.7	3.6
10	3.8	3.7	3.6	3.4	3.3
Total impulse (Ns)	88.7	86.8	84.9	83.1	81.3
Impact downrange (km)	60.06	60.06	60.05	60.05	60.05
impact crossrange (m)	51.29	50.20	49.14	48.09	47.07

Table 4.10: Required side-thruster impulses (Ns) for Cases 6 to 6D.

i^{th} impulse	Case 6A	Case 6B	Case 6	Case 6C	Case 6D
1	31.3	31.3	31.3	31.3	31.3
2	18.2	17.7	17.2	16.8	16.3
3	12.4	12.0	11.6	11.1	10.7
4	9.3	9.0	8.7	8.4	8.0
5	7.4	7.2	6.9	6.7	6.4
6	6.3	6.1	5.9	5.7	5.5
Total impulse (Ns)	85.0	83.2	81.6	79.9	78.3
Impact downrange (km)	60.06	60.06	60.05	60.05	60.05
impact crossrange (m)	51.97	50.89	48.80	48.80	47.48

Table 4.11: Required side-thruster impulses (Ns) for Cases 8 to 8D.

i^{th} impulse	Case 8A	Case 8B	Case 8	Case 8C	Case 8D
1	54.7	54.7	54.7	54.7	54.7
2	20.8	19.9	19.0	18.1	17.3
Total impulse (Ns)	75.5	74.6	73.7	72.8	71.9
Impact downrange (km)	60.06	60.06	60.05	60.05	60.05
impact crossrange (m)	52.20	51.05	49.92	48.81	47.70

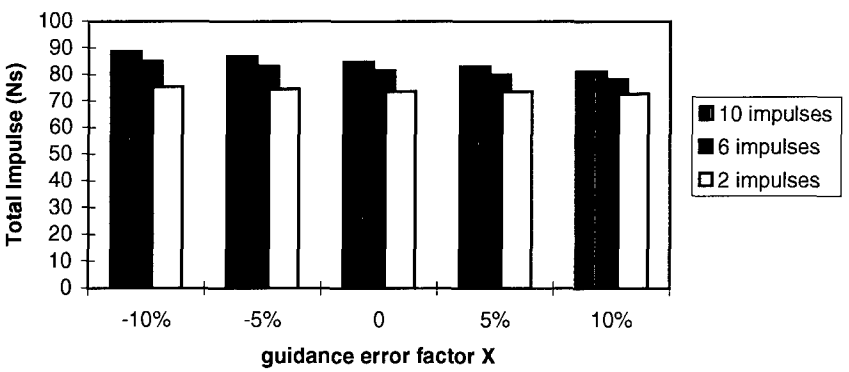

Figure 4.14: Required total side-thruster impulses for different numbers of impulses and guidance error factors (for guidance between burn-out and halfway apogee).

Figure 4.14 shows that for negative guidance error factors, extra impulse is needed to correct the resulting errors in the trajectory. For positive guidance error factors however, the error helps to correct the trajectory; less impulse is needed to achieve a certain correction. This is because for positive values of X, the correcting effect of $(1+X)\cdot\Delta\gamma$ and $(1+X)\cdot\Delta\psi$ in expressions 4.8 and 4.9 on the trajectory is higher than for the situation without guidance error (when $X = 0$). The vehicle is then guided to the target more easily and less impulse is required. For negative values of X, the effect of a side-thruster impulse on the trajectory is diminished, increasing the required impulse.

Additional studies reveal that in the case of two guidance control points, for about $X \geq 1.7$ the total required impulse is also higher than for $X = 0$, because then the

guidance error is so big that the trajectory is 'overguided'. Extra impulse is then necessary to guide the missile to the reference trajectory again.

In Tables 4.9; 4.10 and 4.11 it can be seen that the first impulse is the same for every guidance error factor. This is because the guidance error is not 'known' by the simulation program in advance. When there is a guidance error, the first impulse will not change the trajectory the way it was expected. The guidance will then try to compensate for the error, diminishing or increasing the impulse of the next side-thruster pulse. In the same way, the guidance at every subsequent control point (time of side-thruster pulse) will try to compensate for the guidance error of the previous control point. The guidance error at the last control point cannot however be compensated by subsequent guidance, therefore the coördinates of impact will not be the same as for the case without guidance errors. The differences are small, however.

The total required impulse (for all values of X) increases for higher numbers of impulses, which is in accordance with the results obtained before.
As can be expected, the bigger the guidance error, the higher the increase or decrease of the total impulse. Table 4.11 shows the increase in total impulse as a function of the number of pulses and the guidance error factor X.

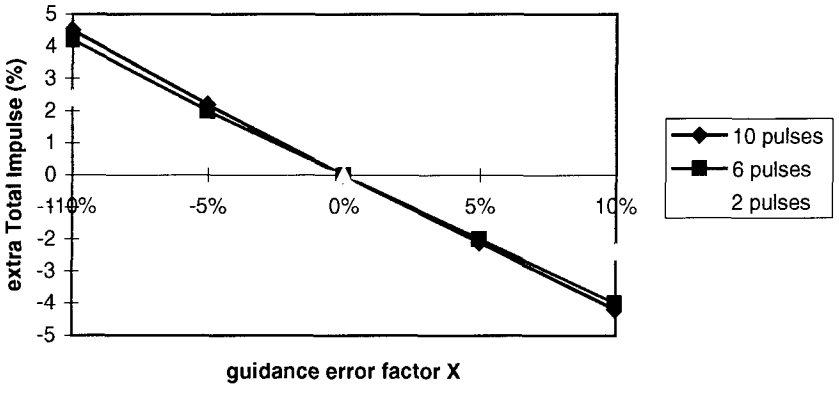

Figure 4.15: Increase percentage in total impulse as a function of the number of pulses and the guidance error factor X.

According to Figure 4.15, the difference (in percentage) in total impulse for a certain guidance error factor decreases for lower numbers of pulses. This is because the less guidance control points, the less guidance errors have to be compensated. Furthermore, the extra total impulse seems to be an almost linear function of the guidance error factor (at least for $-10\% \leq X \leq 10\%$).
Overall, the change in required total impulse for the considered guidance error factors is small.

Effect of guidance errors as a function of the guidance interval

To find out if the guidance interval has an effect on the total impulse for cases with guidance errors, the following cases are studied (all with L = 1.60 m, $x_{c.g.}$ = 1.61 m and two side-thruster pulses):

Cases with guidance between burn-out (t = 0) and quarter-way apogee (t = 11.88 s):

- Case 13A: X = -10%
- Case 13B: X = -5%
- Case 13 : X = 0
- Case 13C: X = 5%
- Case 13D: X = 10%

Cases with guidance between burn-out (t = 0) and halfway apogee (t = 23.75 s):

- Case 8A: X = -10%
- Case 8B: X = -5%
- Case 8 : X = 0
- Case 8C: X = 5%
- Case 8D: X = 10%

Cases with guidance between burn-out (t = 0) and apogee (t = 47.50 s):

- Case 14A: X = -10%
- Case 14B: X = -5%
- Case 14 : X = 0
- Case 14C: X = 5%
- Case 14D: X = 10%

The results are presented in Table 4.17 and Figure 4.16:

Table 4.17: Total impulse as a function of the guidance interval and the guidance error factor X.

Guidance interval X	Burn-out to quarter-way apogee (Case 13)	Burn-out to halfway apogee (Case 8)	Burn-out to apogee (Case 14)
-10%	95.7 Ns	75.5 Ns	82.3 Ns
-5%	93.5 Ns	74.6 Ns	81.6 Ns
0%	91.3 Ns	73.7 Ns	80.8 Ns
5%	89.3 Ns	72.8 Ns	80.1 Ns
10%	87.4 Ns	71.9 Ns	79.4 Ns

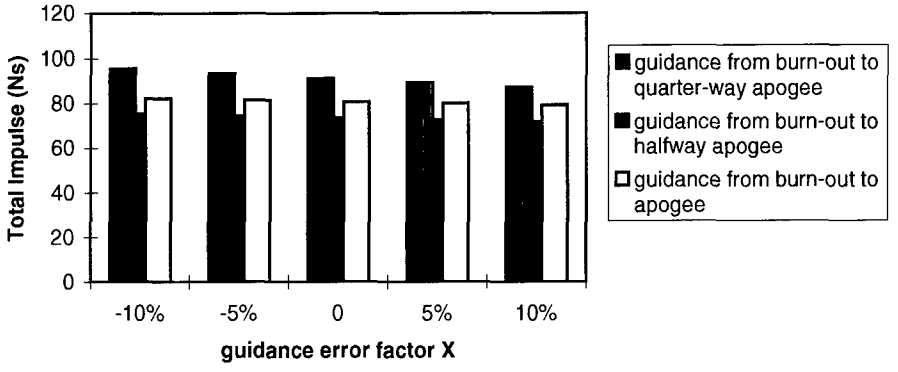

Figure 4.16: Required total side-thruster impulse for different guidance intervals and guidance error factors.

Guidance from burn-out to halfway apogee requires the least total impulse for all guidance error factors, as was expected because of the results presented earlier. The extra total impulse as a function of the guidance error factor is plotted in Figure 4.17:

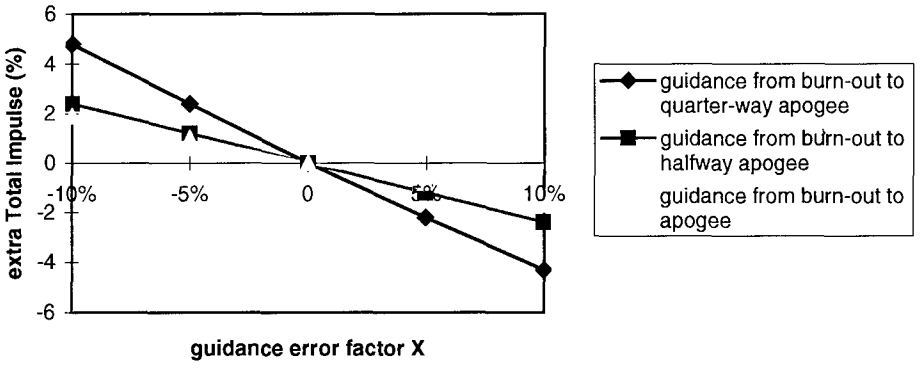

Figure 4.17: Extra total side-thruster impulse for different guidance intervals and guidance error factors.

Again the extra total impulse percentage seems to be a linear function of the guidance error factor X. Although guidance from burn-out to halfway apogee requires the least total impulse for all guidance error factors, the extra total impulse percentage is minimal for guidance from burn-out to apogee. Apparently stretching the guidance interval decreases the extra total impulse percentage.

Effect of extreme guidance errors on the required impulse

As stated before, for extreme high positive values of X, the total required impulse does not decrease anymore because the trajectory is then 'overguided'. Additional study cases (with L = 1.60 m and $x_{c.g.}$ = 1.61 m) result in the graph shown in Figure 4.18.

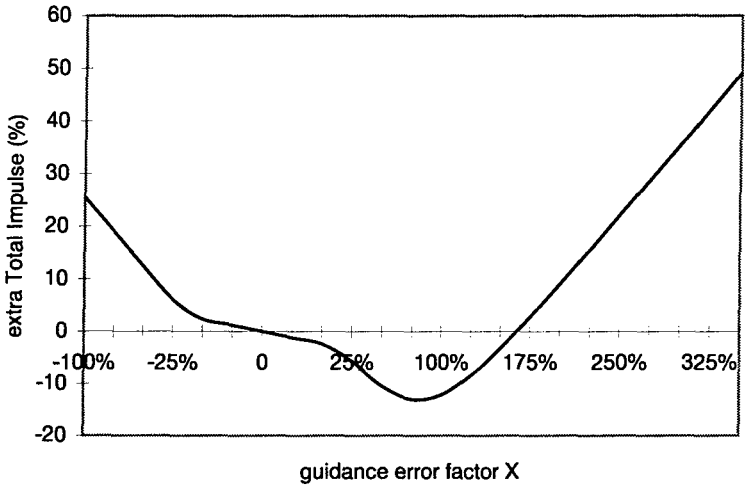

Figure 4.18: Increase percentage in total impulse as a function of the guidance error X (for guidance between burn-out and halfway apogee,two guidance pulses).

From Figure 4.18 it is clear that for error factors higher than 10% or lower than -10% the required extra total impulse is not a linear function of the guidance error factor anymore.

For guidance error factors between 0 and about 80%, the total impulse decreases, because of the increasing correcting effect of $(1+X)\cdot\Delta\gamma$ and $(1+X)\cdot\Delta\psi$ in expressions 2.1 and 2.2 on the trajectory. For $X \approx 80\%$, the trajectory is starting to be 'over-guided', which means $(1+X)\cdot\Delta\gamma$ and $(1+X)\cdot\Delta\psi$ are becoming too high and extra impulse is required to compensate. For about $X = 170\%$, the required total impulse is equal to that required for the case without guidance errors. For higher values of X, guidance requires more impulse than for the case without guidance errors. The required total impulse then increases linearly with the guidance error factor.

For negative values of X, the required total impulse is always higher than for the case without guidance errors. This is because negative X-values diminish the correcting effect of $(1+X)\cdot\Delta\gamma$ and $(1+X)\cdot\Delta\psi$, which means extra impulse is required to guide the vehicle to the reference trajectory.
For values of X lower than about -10%, the necessary extra impulse increases more rapidly than for $-10\% \leq X \leq 0$.

Guidance error factors lower than -10% or higher than 10% are however not very realistic, so assuming $|X| \leq 10\%$, the required total impulse is not very sensitive to guidance errors.

5 Evaluation

Based on the results presented in Chapter 4, several remarks and observations can be made.

Thruster acts through the centre of gravity
The results show that the largest impulses are applied at the start of each chosen guidance time interval. It appears that the impulses applied in Case 4 (time interval from burn-out to halfway apogee) are all smaller than the impulses applied in Cases 1 to 3 (guidance time interval from burn-out to halfway apogee). This implies that the most cost effective guidance is applied in the early phase of the trajectory after burn-out, moreover, the number of pulses does not seem to be important as, the total required impulse is similar for 6, 8 or 10 pulses.

For all guidance cases the order of magnitude of the required side-thruster impulses is realistic. From in-house performed conceptual design studies it followed that a given number of side-thrusters delivering a total impulse of 300 - 500 Ns can be manufactured. With this amount of side-thruster correction, typical errors at burn-out may be reduce to acceptable levels. Furthermore, when the errors at burn-out are smaller, more accuracy at the target is possible.

It has to be kept in mind that in this study only state errors at burn-out are considered as disturbances. When other error sources such as wind and model errors are also taken into account, the results for optimal guidance could change. However, as the linear quadratic regulator is usually a robust guidance concept which can cope with all sort of disturbances [3], the results are still a good indication of what can be expected for the required guidance effort for a range upgraded MLRS-like missile.

Thruster acts not through centre of gravity
The reduction in total required impulse, caused by the aerodynamic forces if the side-thrust is not aimed through the centre of gravity, is quite significant. For the reference vehicle studied in this report, the reduction can be up to about 70% when compared to side-thrust aimed through the c.o.g. of the missile.

To most effectively compensate a burn-out error, guidance should start right after burn-out because the error grows in time and the position of the aerodynamic centre is most optimal right after burn-out.

For a burn-out error, the required total impulse increases slightly for higher numbers of side-thruster burns. This can be explained with the growth of the errors in time; the lower the number of side-thruster pulses, the higher the first impulse at $t = 0$ and thus the more effective the error is compensated. Overall it can be concluded that the number of pulses is not very important for the total impulse.

When the actual missile has different characteristics (e.g. aerodynamics, c.o.g.) than the reference vehicle which is used to guide its trajectory, the resulting guidance error can increase or decrease the required total impulse. The larger the guidance error, the higher the increase/decrease in total impulse.

The required total impulse is not very sensitive to guidance errors.

In case of guidance errors, stretching the guidance interval decreases the extra required total impulse necessary to compensate for the errors.

For all studied cases, the order of magnitude of the required guidance side-thruster impulses is realistic. TNO-PML in-house conceptual design studies revealed that a given number of side-thrusters delivering a total impulse of 300 to 500 Ns (required for guidance with side-thrust aimed through the c.o.g.) can be manufactured and fit well into an MLRS flight vehicle. Side-thrust which is not aimed through the c.o.g. results in lower required total impulses (40 to 180 Ns) and thus a lower demand on the side-thruster system. On the other hand, larger deviations may be corrected as compared to the situation with the side-thruster through the c.o.g..

6 Conclusions and recommendations

By increasing the velocity at burn-out, the 30 km range of an MLRS-type reference vehicle was upgraded to 60 km. To maintain the same accuracy in position at impact as for the 30 km range, the upgraded missile was guided with side-thrusters during the first half of the trajectory (from burn-out until apogee). To study the total impulse required from the side-thruster firings and the effect of side-thruster firings which are not aimed through the centre of gravity, a realistic disturbance case with errors in the burn-out state was used. To determine this disturbance case, a missile with a range of 30 km and an impact just inside an assumed accuracy range of ±50 m in cross- and downrange around the nominal ballistic point of impact was taken as a reference.

Using a linear-quadratic regulator, the upgraded MLRS-type vehicle could be guided so that the same accuracy at impact was achieved as for the 30 km range reference vehicle. For this, a total impulse of 40 to 180 Ns was required when the side-thrusters were positioned in the nose of the vehicle.

The time needed to dampen out the rotation induced by side-thrust which is not aimed through the centre of gravity was studied. The studied guidance cases included a variation of the number of side-thruster firings and the guidance interval. Also several guidance errors were introduced. In all cases, the missile could be guided successfully.

The reduction in required impulse when positioning the side-thrusters in the nose of the vehicle can amount to about 70%. As expected, the largest control effort should be applied at the beginning of the guidance time frame. Applying guidance as early as possible after burn-out is most cost effective; the optimum time-frame to correct burn-out errors is from burn-out to half-way apogee. The guidance is not very sensitive to guidance errors resulting from differing vehicle characteristics.

7 References

[1] Gadiot, G.M.H.J.L.; Marée, A.G.M. and Keus, L.J.,
'Limited sensitivity study on sidfe-thruster guidance for an extended range MLRS-type vehicle',
TNO report PML 1997-A36, August 1997.

[2] Gadiot, G.M.H.J.L.,
'Burnout-to-apogee Guidance Concept for an Artillery Rocket',
Work Description, TNO-PML Internal report,
TNO-G&C-0000-SOW-6/001/I01, 17 April 1996.

[3] Dohrmann, C.R.; Eisler, G.R. and Robinett, R.D.,
'Dynamic Programming Approach for Burnout-to-Apogee Guidance of Precision Munitions',
Journal of Guidance, Control, and Dynamics, Vol. 19, No. 2,
March-April 1996.

[4] Lewis, F.L.,
'Optimal Control',
John Wiley & Sons, New York•Chichester•Toronto•Singapore, 1986.

[5] Ruigrok, G.J.J.,
'Gegevens van de atmosfeer',
Technical University Delft, Faculty of Aerospace Engineering,
Handleiding VTH-71, 1970 (in Dutch).

[6] Gerlach, O.H.,
'Vliegeigenschappen I, deel 1',
Technical University Delft, Faculty of Aerospace Engineering,
Dictaat D 26-I, October 1981 (in Dutch).

[7] Doup, P.W.,
'Summary of the NATO AC/243 DRG Long Term Scientific Study on 'In-expensive Guidance in Indirect Fire Munitions' (LTSS 39)',
TNO report, PML 1993-A93, June 1994.

[8] Yamanaka, T. and Tanaka, H.,
'Effects of Impulse Thruster on Exterior Ballistic Accuracy Improvement for a Hyper Velocity Rocket',
Nissan Motor Co. Ltd., 16th International Symposium on Ballistics, September 1996.

8 Authentication

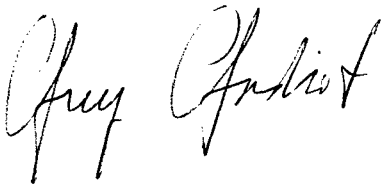

Dr. G.M.H.J.L. Gadiot
Project leader/Author

P.J.M. Elands
Group leader

REPORT DOCUMENTATION PAGE
(MOD-NL)

1. DEFENCE REPORT NO. (MOD-NL)	2. RECIPIENT'S ACCESSION NO.	3. PERFORMING ORGANIZATION REPORT NO.
TD98-0321		PML 1998-A80
4. PROJECT/TASK/WORK UNIT NO.	**5. CONTRACT NO.**	**6. REPORT DATE**
014.10643	A95KL410	May 1999
7. NUMBER OF PAGES	**8. NUMBER OF REFERENCES**	**9. TYPE OF REPORT AND DATES COVERED**
45 (excl. RDP & distribution list)	8	Draft

10. TITLE AND SUBTITLE

Trajectory Simulation Model for a Side-Thruster Guided MLRS-Type Vehicle

11. AUTHOR(S)

Dr. G.M.H.J.L. Gadiot

12. PERFORMING ORGANIZATION NAME(S) AND ADDRESS(ES)

TNO Prins Maurits Laboratory, P.O. Box 45, 2280 AA Rijswijk, The Netherlands
Lange Kleiweg 137, Rijswijk, The Netherlands

13. SPONSORING AGENCY NAME(S) AND ADDRESS(ES)

Ministery of Defence, P.O. Box 90701, 2509 LS The Hague

14. SUPPLEMENTARY NOTES

The classification designation Ongerubriceerd is equivalent to Unclassified.

15. ABSTRACT (MAXIMUM 200 WORDS (1044 BYTE))

This report describes the status of the work carried out by the TNO Prins Maurits Laboratory (TNO-PML) for the Royal Netherlands Army (RNlA) under project A95KL410, titled 'Guidance concepts for indirect fire munitions'. The work is related to the general interest within the military world in extending the range of artillery rocket systems. It is of particular interest to the Royal Netherlands Army who are considering upgrading their existing 30+ km range Multiple Launch Rocket System (MLRS) to a 60 km extended range version. When the range of such a ballistic rocket is upgraded, the effectiveness of these weapons will degenerate if the accuracy in position at impact is not kept at the same level or, preferably, improved. To achieve an improved accuracy the ballistic rocket must be guided to its target.

16. DESCRIPTORS		IDENTIFIERS
Computerized simulation	Trajectories	
Flight simulation	Missiles	
Guidance		
Rocket launchers		
Rocket trajectories		

17a.SECURITY CLASSIFICATION (OF REPORT)	17b.SECURITY CLASSIFICATION (OF PAGE)	17c.SECURITY CLASSIFICATION (OF ABSTRACT)
Ongerubriceerd	Ongerubriceerd	Ongerubriceerd

18. DISTRIBUTION AVAILABILITY STATEMENT	17d.SECURITY CLASSIFICATION (OF TITLES)
Unlimited Distribution	Ongerubriceerd

Distributielijst*

1	DWOO
2	HWO-KL
3*	HWO-KLu
4*	HWO-KM
5*	HWO-CO
6	Ministerie van Defensie, LBBKL Munitiebedrijf, afd. Inkoop en Techniek Maj. ir. J.J. Trouw
7	Ministerie van Defensie, Directie Materieel, Systeemgroep W&T-systemen, Productgroep Gevechtssteun-Materieel
8	DM&P TNO-DO
9*	DM&P TNO-DO, accountcoördinator KL
10*	TNO-FEL, Bibliotheek
11/13	Bibliotheek KMA
14*	Lid Instituuts Advies Raad PML BGen. Prof. J.M.J. Bosch
15*	Lid Instituuts Advies Raad PML Ir. A.H.P.M. Schaeken
16*	Lid Instituuts Advies Raad PML Prof. ir. J.A. Schot
17*	Lid Instituuts Advies Raad PML Prof. ir. K.F. Wakker
18	TNO-PML, Directie; daarna reserve
19	TNO-PML, Hoofd Divisie Munitietechnologie en Explosieveiligheid Ir. P.A.O.G. Korting
20/21	TNO-PML, Divisie Munitietechnologie en Explosieveiligheid, Groep Rakettechnologie Ir. P.J.M. Elands, Dr. ir. G.M.H.J.L. Gadiot
22	TNO-PML, Documentatie
23	TNO-PML, Archief

* De met een asterisk (*) gemerkte instanties/personen ontvangen uitsluitend de titelpagina, het managementuittreksel, de documentatiepagina en de distributielijst van het rapport.